

# Probability of Inflation in Loop Quantum Cosmology

Abhay Ashtekar<sup>1\*</sup> and David Sloan<sup>2,†</sup>

<sup>1</sup> *Institute for Gravitation and the Cosmos, Physics Department,  
Penn State, University Park, PA 16802, U.S.A.*

<sup>2</sup> *Institute for Theoretical Physics, Utrecht University, The Netherlands.*

Inflationary models of the early universe provide a natural mechanism for the formation of large scale structure. This success brings to forefront the question of naturalness: Does a sufficiently long slow roll inflation occur generically or does it require a careful fine tuning of initial parameters? In recent years there has been considerable controversy on this issue [1–4]. In particular, for a quadratic potential, Kofman, Linde and Mukhanov [2] have argued that the probability of inflation with at least 65 e-foldings is close to one, while Gibbons and Turok [4] have argued that this probability is suppressed by a factor of  $\sim 10^{-85}$ . We first clarify that such dramatically different predictions can arise because the required measure on the space of solutions is intrinsically ambiguous in general relativity. We then show that this ambiguity can be naturally resolved in loop quantum cosmology (LQC) because the big bang is replaced by a big bounce and the bounce surface can be used to introduce the structure necessary to specify a satisfactory measure.

The second goal of the paper is to present a detailed analysis of the inflationary dynamics of LQC using analytical and numerical methods. By combining this information with the measure on the space of solutions, we address a sharper question than those investigated in [2, 4, 5]: What is the probability of a sufficiently long slow roll inflation *which is compatible with the seven year WMAP data*? We show that the probability is very close to 1.

The material is so organized that cosmologists who may be more interested in the inflationary dynamics in LQC than in the subtleties associated with measures can skip that material without loss of continuity.

Key Words: Loop quantum gravity, cosmology, inflation, measures, probability, WMAP 7 year data.

## I. INTRODUCTION

The inflationary paradigm provides a natural mechanism of generating the seeds of inhomogeneities in the cosmic microwave background (CMB) which then evolve to the observed, large scale structure of the universe. The general scenario involves a rather small set of assumptions: i) Sometime in its early history, the universe underwent a phase of rapid expansion during which the Hubble parameter was nearly constant; ii) During this phase, the universe was well described by a Friedmann, Lemaître, Robertson, Walker (FLRW) solution

---

\*Electronic address: [ashtekar@gravity.psu.edu](mailto:ashtekar@gravity.psu.edu)

†Electronic address: [sloan@gravity.psu.edu](mailto:sloan@gravity.psu.edu)

to Einstein's equations together with small inhomogeneities which are well approximated by first order perturbations; iii) Consider the co-moving Fourier mode  $k_o$  of perturbations which has just re-entered the Hubble radius now. A few e-foldings before the time  $t(k_o)$  at which  $k_o$  exited the Hubble radius during inflation, Fourier modes of quantum fields describing perturbations were in the Bunch-Davis vacuum for co-moving wave numbers in the range  $(k_o, \sim 200k_o)$ ; and, iv) Soon after a mode exited the Hubble radius, its quantum fluctuation can be regarded as a classical perturbation and evolved via linearized Einstein's equations. Analysis of these perturbations implies that there must be tiny inhomogeneities at the last scattering surface whose detailed features have now been seen in the CMB. Furthermore, time evolution of these tiny inhomogeneities produces large scale structures which are in excellent qualitative agreement with observations. Therefore, even though the assumptions have ad-hoc elements, they appear to capture a germ of truth, not unlike the Bohr atom did a hundred years ago.

For definiteness, let us assume a quadratic potential for the inflaton and supplement our calculations with values of two parameters provided by the seven year WMAP data [6]: the amplitude  $A(t(k_*))$  of the scalar power spectrum  $\Delta_R(t(k_*))$  and the scalar spectral index  $n_S(t(k_*))$  at the time the fiducial mode  $k_*$  used by WMAP exits the Hubble radius ( $k_* \approx 8.58k_o$ ). These numbers, together with the Friedmann equation, determine the values of slow roll parameters and *the initial data for the inflaton and the gravitational field* at time  $t(k_*)$  to within posted observational errors. A slow roll follows and dynamics of perturbations during this epoch directly lead to the spectrum of inhomogeneities seen in the CMB. We will refer to this inflationary phase as the *desired* slow roll to distinguish it from other inflationary phases that may have occurred, e.g., in an even earlier phase.

The striking success of the scenario brings to forefront an old issue in a sharper form: Does the desired slow roll inflation occur generically in a given theoretical paradigm? That is, do generic dynamical trajectories pass through the neighborhood of the values of the inflaton and gravitational fields selected by the WMAP data with its error bars? This would require that the inflaton must have been significantly high up compared to the minimum of the potential at the onset of the desired slow roll. How did it get there? Is it essential to invoke some rare quantum fluctuations to account for the required initial conditions because the a priori probability for their occurrence is low? Or, is the desired slow roll inflation robust in the sense that it is realized in 'almost all' dynamical trajectories of the given theory?

To make these questions precise one needs a well-defined framework to calculate probabilities of various occurrences *within any given theory*. A mathematically natural strategy to achieve this goal was introduced over two decades ago (see e.g. [7–9]). Recall first that the space  $\mathbb{S}$  of solutions to physically interesting classical systems generally carries the natural Liouville measure  $d\mu_L$ . The idea was to calculate *a priori* probabilities using a flat probability distribution  $P(s) = 1$  in conjunction with  $d\mu_L$ . More precisely, the a priori probability of an event  $E$  is given by the *fractional* Liouville volume of  $\mathbb{S}$  occupied by the region  $R(E)$  consisting of solutions on which the event  $E$  is realized [7]. In our case, then, the a priori probability is given by the fractional volume occupied by the sub-space of solutions in which the desired slow roll inflation occurs. Note that this a priori probability provides only a 'bare' estimate and further physical input can and should be used to provide sharper probability distributions  $P(s)$  and a more reliable likelihood. However, a priori probabilities themselves can be directly useful if they are very low or very high. In these cases, it would be an especially heavy burden on the fundamental theory to come up with the physical input that significantly alters them.

However, there is a conceptual obstacle in this calculation: the total Liouville measure of the space  $\mathbb{S}$  of solutions is infinite [9], hence there is an intrinsic ambiguity in the calculation of relative probabilities [3]. But in the observationally favored  $k=0$  FLRW model, this divergence is a gauge artifact. More precisely, a gauge group  $\mathcal{G}$  acts on  $\mathbb{S}$  and, although the quotient  $\mathbb{S}/\mathcal{G}$  —the space of physically distinct solutions— is compact (with boundary), the gauge orbits are non-compact, making the total volume of  $\mathbb{S}$  infinite. It would first appear that the obvious way to avoid the infinite volume is to work directly with the space  $\mathbb{S}/\mathcal{G}$  of physically distinct solutions. However, as we will see, the Liouville measure does not naturally project down to  $\mathbb{S}/\mathcal{G}$ . Therefore, to calculate probabilities, *one has to introduce an additional structure*. Because the subtleties associated with the interplay between the action of the gauge group and the Liouville measure were not well-understood, the necessity and importance of this additional step was, apparently, not appreciated. We will see in section III B that *there is an intrinsic ambiguity in carrying out this step within general relativity*. As a recent analysis of Corichi and Karami [10] shows, this ambiguity is directly related to the diverging conclusions on probability of inflation in general relativity drawn by Koffmann, Linde and Mukhanov [2] and Gibbons and Turok [4].

Loop quantum cosmology (LQC) provides a new arena to analyze this issue because the big bang singularity is naturally resolved and replaced by a big bounce due to quantum geometry effects [11–15]. We will see in section III that, thanks to the presence of a canonical bounce time, one can now naturally resolve the ambiguity in the construction of the measure on  $\mathbb{S}$  with finite total volume. *Were we to try to mimic this construction in general relativity, we would be led to work at the singularity in place of the bounce, where the calculation would be meaningless*. Away from the Planck regime, LQC is virtually indistinguishable from general relativity. However, in the Planck regime, there are huge differences and these are crucial in overcoming the obstacle. With this measure at hand, we can calculate the a priori probability of the slow roll of the desired type. LQC dynamics are such that this probability turns out to be greater than 0.999997: Dynamical trajectories starting from almost all initial data at the bounce surface pass through the phase space region selected by the WMAP data. Therefore, extreme fine tuning would be necessary to zero-in on solutions where the desired slow roll does *not* occur.

Some of the results of our investigation were reported in a Letter [5]. Therefore there is an inevitable overlap with [5] but there are also key differences. First, in [5] we analyzed the likelihood of the occurrence of a slow roll inflation with at least  $\sim 67$  e-foldings in the history of the universe to the future of the bounce. In this paper we analyze a much *sharper question*: What is the probability of occurrence of a slow roll with initial conditions that are compatible with the 7 year WMAP data? Thus we now focus *only* on that slow roll phase which is directly relevant to structure formation. Second, numerical simulations reported in [5] used values of cosmological parameters —the mass of the inflaton and the values of the slow roll parameters— from Linde’s 2006 review [16] while in this paper we use instead the more recent results of the 7 year WMAP data [6]. This accounts for some differences in some of the detailed numerical results. Finally, and more importantly, our goal now is broader than that of [5] in the following sense. In LQC, the big bounce is followed by a qualitatively new phase of super-inflation which could have observable consequences. Therefore, it is important to have a sufficiently detailed account of the new dynamics from the big bounce to the onset of the desired slow roll. A second goal of this paper is to provide this analysis. This detailed description is likely to serve as the point of departure of further work bridging the Planck era of LQC to the inflationary paradigm described in the beginning

of this section. This bridge may, for example, provide a better understanding of why the quantum state of relevant modes is well approximated by the Bunch Davis vacuum at the onset of inflation, and may even furnish the quantum gravity corrections to this state [17].

The paper is organized as follows. In section II we first recall the relevant features of LQC and then introduce the phase space and basic equations. In section III we first introduce the Liouville measure on the space  $\mathbb{S}$  of solutions, discuss the issue of gauge and obtain the measure on the space  $\mathbb{S}/\mathcal{G}$  of physically distinct solutions in LQC. In section IV we discuss in detail the LQC dynamics from the big bounce to the end of inflation using a combination of analytical and numerical methods. Using this information and the measure introduced in section III, we calculate the a priori probability of obtaining the desired slow roll. As noted already, in LQC this probability is very close to 1. Section V summarizes the main results and compares and contrasts them with related results in the literature.

The material is organized so that cosmologists who may be more interested in inflationary dynamics of LQC than in the issue of measures can skip sections IIB and especially III without loss of continuity.

## II. PRELIMINARIES

This section is divided into two parts: In the first, we recall the distinguishing features of LQC that are important to our analysis. In the second, we present effective LQC equations governing dynamics of the FLRW model coupled to a scalar field with any potential (satisfying mild regularity conditions) and introduce the Liouville measure on the space of solutions.

### A. Distinguishing features of LQC

In LQC, one applies the basic principles of loop quantum gravity (LQG) [18–20] to simple cosmological models. Thanks to the quantum geometry underlying LQG, LQC differs from the older Wheeler-DeWitt theory already at the kinematical level. It turns out that the Wheeler-DeWitt equation is no longer well-defined on the new kinematical Hilbert space. Instead, now the quantum Hamiltonian constraint has to be obtained via a procedure that pays due attention to the quantum geometry of LQG, in particular, the area gap  $\Delta = 4\sqrt{3}\pi\gamma\ell_{\text{Pl}}^2$ . (Here  $\gamma$  is the Barbero-Immirzi parameter of LQG, whose value  $\gamma \sim 0.24$  is fixed by black hole entropy calculations [21, 22].) Somewhat surprisingly, the resulting dynamics naturally resolves the big bang and big crunch singularities of general relativity [23]. Exotic matter is not needed; indeed matter fields can satisfy all the standard energy conditions. Detailed analysis has been carried out in a variety of models: the  $k=0, 1$  FLRW space-times with or without a cosmological constant [12–14]; Bianchi models [24–26] which admit anisotropies as well as gravitational waves; and Gowdy models [27] which admit inhomogeneities, and therefore an infinite number of degrees of freedom. The FLRW models have been studied most extensively, using both analytical and numerical methods to solve the exact quantum equations of LQC [12, 13, 15]. In these models, the big bang and the big-crunch are replaced by a quantum bounce, which is followed by a robust phase of super-inflation. Interestingly, full quantum dynamics, including the bounce, is well-approximated by certain effective equations [12, 15, 28]. These equations imply that all strong curvature singularities—including the big rip and sudden-death—are resolved in FLRW models with

matter satisfying an equation of state of the type  $p = w\rho$  [29]. (For recent reviews, see [30].)

In this paper we will restrict our matter source to be a scalar field with the standard (positive) kinetic energy and a suitable potential. Since all the prior discussion of probabilities is based on general relativity, to facilitate comparison we use effective equations rather than the full quantum theory. Finally, we will use the natural Planck units  $c=\hbar=G=1$  (rather than  $8\pi G=1$ , often employed in cosmology). Planck length will be denoted by  $\ell_{\text{Pl}}$  and Planck mass by  $m_{\text{Pl}}$ . The fundamental time unit,  $s_{\text{Pl}} := \sqrt{G\hbar/c^5}$ , will be referred to as *a Planck second*.

In LQC, it is convenient to encode spatial geometry in a variable  $v$  proportional to the physical volume of a fixed, fiducial, cubical cell, rather than the scale factor  $a$ . The conjugate momentum is denoted by  $b$ . These are related to the scale factor and its conjugate momentum via<sup>1</sup>

$$v = \frac{a^3 V_0}{2\pi\gamma} \quad \text{and} \quad b = -\frac{4\pi\gamma P_{(a)}}{3V_0 a^2} \quad (2.1)$$

where  $V_0$  is the co-moving volume of the fiducial cell, so that its physical volume is  $a^3 V_0$ . (Thus, the only non-vanishing Poisson bracket is  $\{v, b\} = -2$ .) On solutions to *Einstein's equations*,  $b$  is related to the standard Hubble parameter  $H = \dot{a}/a$  via  $b = \gamma H$  [15]. However, LQC modifies Einstein dynamics and on solutions to the LQC effective equations we have

$$H = \frac{1}{2\gamma\lambda} \sin 2\lambda b \approx (0.93 m_{\text{Pl}}) \sin 2\lambda b \quad (2.2)$$

where  $\lambda^2 := \Delta \approx 5.2\ell_{\text{Pl}}^2$  is the ‘area-gap’ that sets the discreteness scale of LQC.  $b$  ranges over  $(0, \pi/\lambda)$  in LQC and general relativity is recovered in the limit  $\lambda \rightarrow 0$ .

Quantum geometry effects modify the geometric, left side of Einstein’s equations. In particular, the Friedmann equation becomes

$$\frac{\sin^2 \lambda b}{\gamma^2 \lambda^2} = \frac{8\pi}{3} \rho \equiv \frac{8\pi}{3} \left( \frac{\dot{\phi}^2}{2} + V(\phi) \right). \quad (2.3)$$

To compare with the standard Friedmann equation  $H^2 = (8\pi/3) \rho$ , it is often convenient to use (2.2) to write (2.3) as

$$\frac{1}{9} \left( \frac{\dot{v}}{v} \right)^2 \equiv H^2 = \frac{8\pi}{3} \rho \left( 1 - \frac{\rho}{\rho_{\text{crit}}} \right) \quad (2.4)$$

where  $\rho_{\text{crit}} = 3/8\pi\gamma^2\lambda^2 \approx 0.41\rho_{\text{Pl}}$ . By inspection it is clear from Eqs (2.2) - (2.4) that, away from the Planck regime —i.e., when  $\lambda b \ll 1$ , or,  $\rho \ll \rho_{\text{crit}}$ — we recover classical general relativity. However, modifications in the Planck regime are drastic. The main features of this new physics can be summarized as follows.

- In general relativity, the Friedmann equation implies that if the matter density is positive,  $\dot{a}$  cannot vanish. Therefore every solution represents *either* a contracting universe *or*

---

<sup>1</sup> In LQG, the basic variable is a triad rather than a 3-metric and in the LQC literature  $v$  is taken to be the oriented volume which is positive for positively oriented triads and negative for negatively oriented ones. However, since the change of orientation is a large gauge transformation, in the classical and effective theories one can restrict oneself just to positive  $v$ . We have done so for simplicity of discussion.

an expanding one. By contrast, the LQC modified Friedmann equation (2.4) implies that  $\dot{v}$  vanishes at  $\rho = \rho_{\text{crit}}$ . This is the quantum bounce. To its past, the solution represents a contracting universe with  $\dot{v} < 0$  and to its future, an expanding one with  $\dot{v} > 0$ .

- As is customary in the literature on probabilities, let us ignore the exceptional de Sitter solutions. On all other solutions  $b$  is monotonically non-increasing, evolving from  $b = \pi/\lambda$  in the infinite past to 0 in the infinite future. Eqs (2.3) and (2.4) imply that  $b = \pi/2\lambda$  at the bounce. Thus, each solution undergoes precisely one bounce.

- In contrast to general relativity, the Hubble parameter  $H = \dot{v}/3v$  is no longer monotonic in LQC. It *vanishes* at the bounce while in general relativity it diverges at the singularity and is large in the entire Planck regime. In LQC,  $H$  is bounded above,  $|H| \lesssim 0.93 m_{\text{Pl}}$ , and achieves its upper bound in every solution at the end of super-inflation.

- If the potential  $V(\phi)$  is bounded below, say  $V \geq V_o$ , then it follows from (2.3) that  $\dot{\phi}^2$  is bounded by  $2\rho_{\text{crit}} - 2V_o$ . If  $V$  grows unboundedly for large  $|\phi|$ , then  $|\phi|$  is also bounded. For example, for  $V = m^2\phi^2/2$ , we have  $m|\phi|_{\text{max}} = 0.90 m_{\text{Pl}}^2$ .

- When the potential is bounded below,  $|\dot{H}|$  is bounded above by  $10.29 m_{\text{Pl}}^2$ . The Ricci scalar —the only non-trivial curvature scalar in these models— is bounded above by  $31m_{\text{Pl}}^2$ . Thus, physical quantities which diverge at the big bang of general relativity cannot exceed certain finite, maximum values in LQC. One can also show that if  $v \neq 0$  initially, it cannot vanish in finite proper time along any solution. Thus, *the LQC solutions are everywhere regular irrespective of whether one focuses on matter density, curvature or the scale factor.*

## B. The Liouville measure

The full set of space-time equations of motion can be written in terms of  $v(t), \phi(t)$ . These variables are subject to the constraint (2.4) and evolve via:

$$\ddot{v} = \frac{24\pi v}{\rho_{\text{crit}}} [(\rho - V(\phi))^2 + V(\phi)(\rho_{\text{crit}} - V(\phi))] \quad (2.5)$$

$$\ddot{\phi} + \frac{\dot{v}}{v} \dot{\phi} + V_{,\phi} = 0. \quad (2.6)$$

To calculate probabilities, in section III we have to equip the space  $\mathbb{S}$  of solutions to these equations with a natural measure. As a first step in that procedure, we will now obtain a phase space formulation of these equations. The phase space and equations of general relativity can be recovered by taking the limit  $\lambda \rightarrow 0$  (which in particular implies  $\rho_{\text{crit}} \rightarrow \infty$ ).

The phase space  $\Gamma$  consists of quadruplets  $(v, b; \phi, p_\phi)$ , where  $p_\phi$  is given by;  $p_\phi = 2\pi\gamma\ell_{\text{Pl}}^2 v \dot{\phi}$ . The variables  $\phi, p_\phi$  range over the entire real line,  $v$  over the positive half of the real line, while  $b \in [0, \pi/2\lambda]$  (since we focus only on the post-bounce branches of solutions). Thus, the symplectic 2-form is given by

$$\Omega = d\phi \wedge dp_\phi + \frac{1}{2}db \wedge dv \quad (2.7)$$

Hence the Liouville measure on  $\Gamma$  is simply  $2d\mu_{\text{L}} = d\phi dp_\phi db dv$ .

The LQC Friedmann equation implies that these variables must lie on a constraint surface  $\bar{\Gamma}$  defined by

$$C \equiv -\frac{3v}{4\gamma\lambda^2} \sin^2 \lambda b + \frac{p_\phi^2}{4\pi\gamma v} + 2\pi\gamma v V(\phi) \approx 0. \quad (2.8)$$

They evolve via

$$\dot{v} = \frac{3v}{2\gamma} \frac{\sin 2\lambda b}{\lambda}, \quad \dot{b} = -\frac{p_\phi^2}{\pi\gamma v^2}, \quad (2.9)$$

$$\dot{\phi} = \frac{p_\phi}{2\pi\gamma v}, \quad \dot{p}_{(\phi)} = -2\pi\gamma v V_{,\phi}. \quad (2.10)$$

As is well-known, the space of solutions  $\mathbb{S}$  is naturally isomorphic to a gauge-fixed surface, i.e., a 2-dimensional surface  $\hat{\Gamma}$  of  $\bar{\Gamma}$  which is intersected by each dynamical trajectory once and only once. Since  $b$  is monotonic in each solution, an obvious strategy is to choose for  $\hat{\Gamma}$  a 2-dimensional surface  $b = b_o$  (a fixed constant) within  $\bar{\Gamma}$ .

It is straightforward to pull-back the symplectic structure to this 2-dimensional gauge-fixed surface  $\hat{\Gamma}$ . Using the constraint (2.8), it is convenient to coordinatize  $\hat{\Gamma}$  using  $v, \phi$  and express the pulled-back symplectic structure in terms of them:

$$\hat{\Omega} = \left[ \frac{3\pi}{\lambda^2} \sin^2 \lambda b_o - 8\pi^2 \gamma^2 V(\phi) \right]^{\frac{1}{2}} d\phi \wedge dv \quad (2.11)$$

This 2-form provides a Liouville measure  $d\hat{\mu}_L$  on  $\hat{\Gamma}$  and hence of the space  $\mathbb{S}$  of solutions to the effective equations, given simply by

$$d\hat{\mu}_L = \left[ \frac{3\pi}{\lambda^2} \sin^2 \lambda b_o - 8\pi^2 \gamma^2 V(\phi) \right]^{\frac{1}{2}} d\phi dv. \quad (2.12)$$

The most natural choice in LQC is to set  $b_o = \pi/2\lambda$  so that  $\bar{\Gamma}$  is just the ‘bounce surface’. We will make this choice because it also turns out to be convenient for calculations. However, since the dynamical flow preserves the symplectic structure on  $\Gamma$ , this measure on  $\mathbb{S}$  is insensitive to the choice of  $b_o$  used in gauge fixing.

### III. PROBABILITY CONSIDERATIONS

Recall from section I that the a priori probability of occurrence of any event  $E$  is to be given by the fractional volume of the region  $R(E)$  in  $\mathbb{S}$  spanned by solutions in which  $E$  occurs:

$$P(E) = \frac{\int_{R(E)} d\hat{\mu}_L}{\int_{\mathbb{S}} d\hat{\mu}_L}. \quad (3.1)$$

Since the Liouville measure is purely kinematical, this method of calculating a priori probabilities realizes Laplace’s *principle of indifference* [31]. This interpretation can be made explicit as follows. Physical input can provide a (non-negative) probability density function  $\rho(s)$  on  $\mathbb{S}$  satisfying the normalization condition  $[\int_{\mathbb{S}} \rho d\hat{\mu}_L] / [\int_{\mathbb{S}} d\hat{\mu}_L] = 1$ . The corresponding (more refined) probability of occurrence of  $E$  is then given by

$$P_\rho(E) = \frac{\int_{R(E)} \rho(s) d\hat{\mu}_L}{\int_{\mathbb{S}} \rho(s) d\hat{\mu}_L}. \quad (3.2)$$

Now, one can quantify the information contained in  $\rho(s)$  via

$$I_\rho = \frac{\int_{\mathbb{S}} \rho(s) \ln \rho(s) d\hat{\mu}_L}{\int_{\mathbb{S}} \rho(s) d\hat{\mu}_L}. \quad (3.3)$$

Since  $I$  is minimized by  $\rho(s) = 1$ , (3.1) is the *a priori* probability, free of any input or bias. As mentioned in section I, these ‘bare’ probabilities are useful when they are extremely low or extremely high. In these cases it is a heavy burden on any theory to provide sufficient information to significantly overcome this bare probability.

In section III A we illustrate these ideas using a 2-dimensional simple harmonic oscillator constrained to have a fixed energy. In this case the solution space  $\mathbb{S}$  is compact. Since the total Liouville volume of  $\mathbb{S}$  is finite, one can directly implement the ideas outlined above to calculate various probabilities. In section III B we turn to LQC. In this case,  $\mathbb{S}$  is non-compact. But we will see that this non-compactness can be directly attributed to the action of a gauge group  $\mathcal{G}$  on  $\mathbb{S}$ . Therefore, it is now natural to work with the space  $\tilde{S} := \mathbb{S}/\mathcal{G}$  of physically distinct solutions which is compact. However, there is a subtlety which makes the calculation of desired probabilities ambiguous in general relativity. We discuss this problem and show that it has a natural resolution in LQC.

Cosmologists who are more interested in the LQC dynamics than in the issue of measure on  $\mathbb{S}$  can skip section III without loss of continuity.

### A. Harmonic oscillator

Since we encounter a constrained Hamiltonian system both in general relativity and (effective) LQC, let us begin with a simple example with this feature to illustrate the procedure of calculating probabilities. Consider a 2-dimensional simple harmonic oscillator constrained to have a fixed energy  $E$ . Let us fix the mass and spring constant to unity for simplicity. The topology of our phase-space  $\Gamma$  is then  $\mathbb{R}^4$ , in which we can choose canonical coordinates  $x_1, p_1; x_2, p_2$ , with symplectic structure:

$$\omega = dx_1 \wedge dp_1 + dx_2 \wedge dp_2 \quad (3.4)$$

The Hamiltonian constraint is:

$$H := \frac{1}{2}(x_1^2 + p_1^2 + x_2^2 + p_2^2) = E \quad (3.5)$$

The constrained surface  $\bar{\Gamma}$  is the 3-sphere with radius  $\sqrt{2E}$  in  $\mathbb{R}^4$  and thus compact. The Hamiltonian vector field is given by

$$X_H = x_1 \frac{\partial}{\partial p_1} - p_1 \frac{\partial}{\partial x_1} + x_2 \frac{\partial}{\partial p_2} - p_2 \frac{\partial}{\partial x_2} \quad (3.6)$$

The vector field is of course tangential to  $\bar{\Gamma}$  and its orbits provide a Hopf fibration: each orbit is an  $S^1$  fiber with the base space being  $S^2$ . This base space represents the space  $\mathbb{S}$  of solutions of the constrained system under consideration.

It is convenient to use a set of coordinates adapted to this Hopf fibration:

$$x_1 + ip_1 = \sqrt{2E} e^{i\xi_1} \sin \eta \equiv z_1 \quad \text{and} \quad x_2 + ip_2 = \sqrt{2E} e^{i\xi_2} \cos \eta \equiv z_2 \quad (3.7)$$

where  $\eta \in (0, \pi/2)$  and  $\xi_1, \xi_2 \in (0, 2\pi)$ . Then  $\bar{\Gamma}$  is given by  $|z_1|^2 + |z_2|^2 = 2E$  and the angles  $\eta, \xi_1, \xi_2$  provide a natural set of intrinsic coordinates on it. The pull-back  $\bar{\Omega}$  of  $\Omega$  to  $\bar{\Gamma}$  can now be expressed as

$$\bar{\Omega} = 2E \sin 2\eta \, d\eta \wedge d\xi^- \quad (3.8)$$



and the restriction of the Hamiltonian vector field to  $\bar{\Gamma}$  is given by

$$\bar{X}_H = 2 \frac{\partial}{\partial \xi^+} \quad (3.9)$$

where we have set  $2\xi^\pm = \xi_1 \pm \xi_2$ . As expected,  $\bar{\Omega}$  is degenerate and the degenerate direction is precisely  $\bar{X}_H$ . It is obvious that  $\eta, \xi^-$  and  $\bar{\Omega}$  are Lie dragged by  $\bar{X}_H$ . Hence they have unambiguous projections to the 2-sphere of orbits of  $\bar{X}_H$ , i.e., to the space  $\mathbb{S}$  of solutions. The total Liouville volume of  $\mathbb{S}$  is given by:

$$\int_{\mathbb{S}} \bar{\Omega} = 2E \int_0^{\pi/2} d\eta \sin 2\eta \int_0^{2\pi} d\xi^- = 2\pi(2E). \quad (3.10)$$

We can now use the Liouville measure  $d\mu_L = (2E) \sin 2\eta d\eta d\xi^-$  on  $\mathbb{S}$  to calculate the a priori probabilities of physical events of interest. Consider example, the total angular momentum

$$J := x_1 p_2 - x_2 p_1 = -E \sin 2\eta \sin 2\xi^- \quad (3.11)$$

which is a Dirac observable and thus projects down from  $\Gamma$  to  $\mathbb{S}$  unambiguously. Another Dirac observable is the eccentricity of the orbit in  $x_1, x_2$  plane defined in each solution,  $e = r_{\min}/r_{\max}$  where  $r^2 = x_1^2 + x_2^2$ . One can show that  $e$  is determined completely by the ratio  $|J|/E$ :

$$e = \frac{r_{\min}}{r_{\max}} = \sqrt{\frac{1 - \sqrt{1 - \frac{J^2}{E^2}}}{1 + \sqrt{1 - \frac{J^2}{E^2}}}}. \quad (3.12)$$

To gain insight into the likelihood of various values for both observables, it is natural to ask, e.g., for the a priori probability that  $|J|/E$  is larger than a given number  $f \in [0, 1]$ . We obtain :

$$P(|J|/E > f) = \frac{1}{4\pi E} \int_A \bar{\Omega} = 1 - f \quad (3.13)$$

where  $A$  is the region such that  $\sin 2\eta \sin 2\xi^- > f$ . We find that the probability for  $e > 1/2$  is  $P_{|J|/E > 16/25} = 1 - 16/25 = 9/25$  and the probability for  $e > 3/4$  is only  $49/625 \approx 0.08$ . We can therefore conclude that almost circular orbits ( $e \approx 1$ ) are rare according to our measure, and thus if the orbit of a particle in this system were observed to be very close to circular, further physical explanation would be required.

Finally, in this analysis we identified the solution space  $\mathbb{S}$  with the quotient of  $\bar{\Gamma}$  by the orbits of the Hamiltonian vector field. In general relativity and LQC it is more convenient to gauge fix. In the present case, because the orbits of  $X_H$  provide a Hopf fibration of  $\bar{\Gamma}$  a global gauge fixing is not available. Still, for calculating probabilities, we can ignore sets of measure zero and parameterize  $\mathbb{S}$  by points of a 2-dimensional surface  $\hat{\Gamma}$  given by  $\xi^+ = \text{const}$ . For physical questions such as the ones discussed above, the resulting a priori probabilities are insensitive to the choice of the constant and the results are the same as those obtained above.

## B. Measures for general relativity and LQC

Recall from section II that the phase space  $\Gamma$  of LQC is naturally coordinatized by  $(v, b; \phi, p_\phi)$  where  $v$  takes values in the positive half line,  $\phi, p_\phi$  on  $\mathbb{R}$  and  $b \in (0, \pi/\lambda)$ . These

phase space variables are subject to the Hamiltonian constraint (2.8) of effective LQC and dynamics of this theory is generated by the Hamiltonian vector field  $X_C$  of the constraint function  $C$ :

$$X_C = \left(\frac{3v}{2\gamma} \frac{\sin 2\lambda b}{\lambda}\right) \frac{\partial}{\partial v} - \left(\frac{p_\phi^2}{\pi\gamma v^2}\right) \frac{\partial}{\partial b} + \left(\frac{p_\phi}{2\pi\gamma v}\right) \frac{\partial}{\partial \phi} - (2\pi\gamma v V_{,\phi}) \frac{\partial}{\partial p_\phi}. \quad (3.14)$$

There is a gauge symmetry which will play an important role in our probability considerations. Since  $v$  is, by definition, the physical volume of a fiducial cell and the choice of this cell is arbitrary, physics does not change under the transformation

$$(v, b; \phi, p_\phi) \longrightarrow (\alpha v, b; \phi, \alpha p_\phi) \quad (3.15)$$

which corresponds merely to a rescaling of the fiducial cell by a positive number  $\alpha$  (recall:  $p_\phi = 2\pi\gamma\ell_{\text{Pl}}^2 v \dot{\phi}$ ). Thus the phase space  $\Gamma$  is acted upon by the action of a gauge group  $\mathcal{G}$  generated by (3.15). (This gauge freedom is equivalent to that in rescaling the scale factor in the more familiar Wheeler-DeWitt phase space.) At an infinitesimal level this rescaling defines a vector field

$$G = v \frac{\partial}{\partial v} + p_\phi \frac{\partial}{\partial p_\phi}. \quad (3.16)$$

Under this rescaling the constraint function (2.8) and the symplectic structure (2.7) are merely rescaled,  $\mathcal{L}_G C = C$  and  $\mathcal{L}_G \Omega = \Omega$ , such that the Hamiltonian vector field (3.14) is left invariant,  $\mathcal{L}_G X_C = 0$ . Hence, as one would expect of gauge transformations,  $\mathcal{G}$  descends to the space  $\mathbb{S}$  of solutions. These considerations hold both for effective LQC and general relativity.

Next, let us find a suitable parametrization of  $\mathbb{S}$ . Note first that we can solve (2.8) for  $p_\phi$ :

$$p_\phi = \pm \left[ \frac{3\pi v^2}{\lambda^2} \sin^2 \lambda b - 8\pi^2 \gamma^2 v^2 V(\phi) \right]^{1/2}. \quad (3.17)$$

Without loss of generality we can restrict ourselves to the positive branch  $p_\phi \geq 0$  because identical considerations will apply to the negative branch. Thus the constraint surface  $\bar{\Gamma}$  is coordinatized by  $(v, b, \phi)$ . Since the dynamical trajectories lie in  $\bar{\Gamma}$ , the space of solutions  $\mathbb{S}$  is 2-dimensional and naturally isomorphic to any gauge-fixed surface  $\hat{\Gamma}$  in  $\bar{\Gamma}$  which is intersected by each dynamical trajectory once and only once. Since  $b$  is monotonic along dynamical trajectories, we can take  $\hat{\Gamma}$  to be the 2-dimensional surface  $(v, b = b_o, \phi)$  for any fixed constant  $b_o$  in the domain  $(0, \pi/\lambda)$  of  $b$ .<sup>2</sup> The Liouville measure  $d\hat{\mu}_L$  on  $\hat{\Gamma}$ , and hence on  $\mathbb{S}$ , is then given by (2.12):

$$d\hat{\mu}_L = \left[ \frac{3\pi}{\lambda^2} \sin^2 \lambda b_o - 8\pi^2 \gamma^2 V(\phi) \right]^{\frac{1}{2}} d\phi dv. \quad (3.18)$$

Since it is induced by the symplectic structure, the  $d\hat{\mu}_L$  volume of any region on the  $b = b_o$  section is the same as that of its image on any other  $b = \text{const}$  surface under the Hamiltonian flow  $X_C$ . In this sense,  $d\hat{\mu}_L$  is insensitive to the choice of  $b_o$ . The analogous structures

---

<sup>2</sup> It is then convenient to choose the freedom in rescaling the constraint —i.e., in the choice of the lapse function— to make  $b$  the affine parameter of the Hamiltonian vector field, so that  $X_C$  now maps each  $b = \text{const}$  surface to another  $b = \text{const}$  surface.

$\Gamma_{\text{GR}}, \bar{\Gamma}_{\text{GR}}, \hat{\Gamma}_{\text{GR}}$  and  $d\hat{\mu}_{\text{L}}^{\text{GR}}$  in general relativity are obtained by taking the limit  $\lambda \rightarrow 0$ . In particular, in this limit  $b \rightarrow H$ , the Hubble parameter. Hence in general relativity one can naturally fix the gauge by setting  $H = H_o$  for any positive constant  $H_o$ .

The essential problem in both cases is that the spaces of solutions  $\mathbb{S}$  and  $\mathbb{S}_{\text{GR}}$  are non-compact and their volume with respect to  $d\hat{\mu}_{\text{L}}$  and  $d\hat{\mu}_{\text{L}}^{\text{GR}}$  is infinite. Therefore we cannot directly use the procedure of section III A to calculate probabilities of events of interest. Let us restrict ourselves to positive potentials  $V(\phi)$ —such as the quadratic and quartic ones which are often analyzed in detail— which diverge at  $\phi = \pm\infty$ . Then the constraint (2.8) (and its GR analog, the Friedmann equation) immediately implies that *the range of  $\phi$  is bounded* on  $\hat{\Gamma}$ . Thus, the non-compactness of  $\hat{\Gamma}$  and  $\hat{\Gamma}_{\text{GR}}$  arises only because  $v$  ranges over the entire positive real line. However, as we saw in the beginning of this sub-section, the transformation  $(v, \phi) \rightarrow (\alpha v, \phi)$  is a gauge motion. Thus, the total Liouville measure of  $\mathbb{S}$  is infinite simply because each orbit of the gauge group  $\mathcal{G}$  is infinitely long.

Let us spell out the interaction between the gauge group and the space of solutions  $\mathbb{S}$  explicitly. Since  $\mathcal{L}_G C = 0$ , the gauge vector field  $G$  is tangential to  $\bar{\Gamma}$ . Furthermore since  $\mathcal{L}_G b = 0$  (and  $\mathcal{L}_G H = 0$  in general relativity),  $G$  is also tangential to the gauge-fixed surface  $b = b_o$  in effective LQC (and to the gauge-fixed surface  $H = H_o$  in general relativity). Thus,  $G$  is tangential to  $\hat{\Gamma}$  (and  $\hat{\Gamma}_{\text{GR}}$ ), i.e., the action of the gauge group  $\mathcal{G}$  naturally respects our parametrization of the space  $\mathbb{S}$  of solutions using  $\hat{\Gamma}$ . The space of *physically distinct* solutions is the quotient  $\tilde{\mathbb{S}} := \mathbb{S}/\mathcal{G}$ , coordinatized just by  $\phi$  which takes values on a compact interval, say  $(\phi_{\min}, \phi_{\max})$ . Since we are interested in gauge invariant questions, regions  $R(E)$  of  $\mathbb{S}$  consisting of solutions in which *physical* events—such as the desired slow roll inflation— occur contain whole orbits of  $\mathcal{G}$  and project down unambiguously to  $\tilde{\mathbb{S}}$ . To calculate the probability of such events, then, it would suffice to have available a natural measure on  $\tilde{\mathbb{S}}$ . Since  $\tilde{\mathbb{S}}$  is a closed interval, one would expect a natural construction to provide it with a finite total measure, making the calculation of desired probabilities well-defined as in section III A.

Thus, the natural strategy is to attempt to introduce a volume element on  $\tilde{\mathbb{S}} = \hat{\Gamma}/\mathcal{G}$  starting from the symplectic structure  $\hat{\Omega}$  on  $\hat{\Gamma}$ .<sup>3</sup> The obvious candidate for such a volume element is the natural 1-form  $\hat{\omega}_\alpha = \hat{\Omega}_{\alpha\beta} G^\beta$  which is transverse to the gauge direction  $G^\alpha$ . Unfortunately, since  $\mathcal{L}_G \hat{\omega}_\alpha = (\mathcal{L}_G \hat{\Omega}_{\alpha\beta}) G^\beta = \hat{\omega}_\alpha \neq 0$ , this 1-form  $\hat{\omega}_\alpha$  does *not* project down to  $\tilde{\mathbb{S}}$ . Therefore to implement this strategy one has to introduce an additional structure. Let us fix a line  $\mathbb{S}_o$  in  $\mathbb{S} = \hat{\Gamma}$  given by  $v = v_o$  for some constant  $v_o$ , which is naturally isomorphic to  $\tilde{\mathbb{S}} = \hat{\Gamma}/\mathcal{G}$ .<sup>4</sup> One can then just pull-back the 1-form  $\hat{\omega}$  to  $\mathbb{S}_o$  and perform integrations there. Expression (2.11) of  $\hat{\Omega}$  implies that the total volume of  $\mathbb{S}_o$  is given by

$$\int_{\mathbb{S}_o} \hat{\omega} = \int_{-\phi_{\max}}^{\phi_{\max}} \left( \frac{3\pi}{\lambda^2} \sin^2 \lambda b_o - 8\pi^2 \gamma^2 V(\phi) \right)^{\frac{1}{2}} v_o d\phi, \quad (3.19)$$

which is manifestly finite. Finally, a change in the value of  $v_o$  would simply rescale  $\hat{\omega}$  by

<sup>3</sup> A straightforward push-forward of the Liouville measure  $\hat{\mu}_{\text{L}}$  on  $\mathbb{S} = \hat{\Gamma}$  is not useful because it would assign to any interval on  $\hat{\Gamma}/\mathcal{G}$  the same volume as its inverse image in  $\hat{\Gamma}$  which is infinite.

<sup>4</sup> The use of a more general line,  $v = f(\phi)$ , would correspond to giving the gauge orbits a  $\phi$  dependent regularized volume. This would introduce an ad-hoc new input in the construction. With  $v = v_o$ , the regularized volume of each orbit is the same and, as explained below, it drops out in the calculation of probabilities of physical events.

a *constant*. Since the relative probability  $P(E)$  of the occurrence of a physical event  $E$  is given by

$$P(E) = \frac{\int_{\mathcal{I}(E)} \hat{\omega}}{\int_{\mathbb{S}_o} \hat{\omega}}, \quad (3.20)$$

where  $\mathcal{I}(E)$  is the intersection of the  $v = v_o$  line and the region  $R(E)$  on which the property  $E$  is realized, clearly,  $P(E)$  is independent of the choice of  $v_o$  made above.

Thus, it would appear that we have satisfactorily eliminated the spurious infinity in the total Liouville measure and arrived at a natural procedure to calculate desired probabilities. However, there is an important subtlety which makes the procedure ambiguous. Recall that in order to arrive at  $\hat{\omega}$  we made *two* gauge choices: We set  $b = b_o$  (or,  $H = H_o$  in GR) and then  $v = v_o$ . The symplectic structure and the 1-form  $\hat{\omega}$  on  $\mathbb{S}$  is preserved by the Hamiltonian flow and (with the appropriately chosen lapse) the flow maps each of our 2-dimensional gauge fixed surfaces  $b = \text{const}$  to another such surface. However, under this flow, the data  $(v = v_o, b = b_o; \phi, p_\phi = p_\phi(v_o, b_o, \phi))$  with constant  $v$  on the  $b = b_o$  slice is *not* mapped to data with constant  $v$  at another slice, say  $b = b_1$ . (Here  $p_\phi(v_o, b_o, \phi)$  is the solution (3.17) of the constraint). Therefore the final step, where we carry out the integration on the  $v = v_o$  line, of our procedure sensitively depends on our initial choice of  $b_o$  (or  $H = H_o$  in general relativity). The question then is: Is there a canonical choice  $b_o$  one can make in LQC (or,  $H_o$  in general relativity)?

In general relativity, the answer is in the negative: there is no preferred value of the Hubble parameter or a canonical instant of time in any solution. Therefore the calculation of probabilities has an intrinsic ambiguity. Although there are also other differences (discussed in section V), this ambiguity lies at the source of dramatically different predictions on the probability of inflation because, in effect, by choosing very different values of  $H_o$ , one can arrive at very different measures for computing probabilities. In terms of these considerations, Gibbons and Turok chose a low value of  $H_o$  and found that the sub-space of solutions admitting a sufficiently long slow roll occupies an extremely tiny relative volume of  $\mathbb{S}$  with respect to the resulting measure on  $\mathbb{S}$ . A higher value of  $H_o$ —as was advocated in the early literature (see, e.g. [32])—increases this probability very substantially. In LQC, on the other hand, the bounce surface provides a canonical ‘time’ instant, i.e., a natural value for  $b_o$ , namely  $b_o = \pi/2\lambda$  where the matter density attains its maximum value. The corresponding surface in general relativity would be the big bang singularity and, unfortunately, we cannot use the ‘data at the big bang’ to parameterize the space  $\mathbb{S}$  of solutions.<sup>5</sup>

To summarize, as discussed in the early literature [7–9], the Liouville measure on the phase space naturally descends to the space  $\mathbb{S}$  of solutions but the total  $d\hat{\mu}_L$  measure of  $\mathbb{S}$  is infinite. In the observationally favored  $k=0$  models this infinity is physically spurious because it arises only because the length of gauge orbits is infinite. For physical questions one can work with the quotient  $\mathbb{S}/\mathcal{G}$  which is just a bounded interval of the real line both in general relativity and LQC. However, although the Hamiltonian vector field  $X_C$  is invariant under the action of the gauge group  $\mathcal{G}$ , the symplectic structure is not. Consequently, the Liouville measure fails to naturally descend to a measure (with finite total volume) on  $\mathbb{S}/\mathcal{G}$ . To introduce such a measure, an additional structure is needed. Because of the presence of

---

<sup>5</sup> A common suggestion that one should carry out the calculation when the Hubble parameter is of Planck scale, rather than infinite, comes close to the natural strategy in LQC but the suggestion is only qualitative and, strictly speaking, quite different because in LQC the Hubble parameter vanishes at the bounce surface.

the bounce, this structure is naturally available in LQC. In general relativity, by contrast, there does not appear to exist a natural way to introduce the required structure; the analog of the bounce surface would be the big bang singularity itself! Consequently, in general relativity, the calculation of a priori probabilities of various physical events along the lines of [7–9] is intrinsically ambiguous.

*Remark:* In LQC, the final result can be stated directly in terms of the Liouville measure  $d\hat{\mu}_L$  on  $\mathbb{S} = \hat{\Gamma}$ . The regions of interest  $R(E)$  spanned by solutions in which a physical event  $E$  occurs contain whole orbits of the gauge group  $\mathcal{G}$ :  $R(E) = I \times \mathbb{R}^+$  where  $I$  is a closed interval in  $[-\phi_{\max}, \phi_{\max}]$  and  $\mathbb{R}^+$  denotes the  $v$  axis ( $\phi$  and  $v$  evaluated at the bounce surface  $b = \pi/2\lambda$ ). The associated probability  $P(E)$  is given by first introducing a ‘slab’  $I_{v_o}$  in the 2-dimensional space  $\hat{\Gamma}$ , bounded by  $v = v_o$  and  $v = 1/v_o$  with  $0 < v_o < 1$ , and then taking the limit  $v_o \rightarrow 0$ :

$$P(E) = \lim_{v_o \rightarrow 0} \frac{\text{Liouville Volume of } [I \times I_{v_o}]}{\text{Liouville Volume of } [I_{\text{total}} \times I_{v_o}]} \quad (3.21)$$

This is the expression that was used in [5].

#### IV. INFLATIONARY DYNAMICS IN LQC

The event  $E$  of interest to us is the presumed slow roll that is compatible with the WMAP data. With a canonical measure on the space  $\mathbb{S}/\mathcal{G}$  of physically distinct solutions of LQC at hand, we can now ask for the relative volume occupied by the region  $R(E)$  consisting of solutions in which  $E$  occurs. In this section we will first characterize this subspace by analyzing in detail the post-bounce dynamics of LQC and then calculate its relative volume.

In section IV A we collect useful facts about the desired slow roll that are used throughout the subsequent subsections. Solutions of effective LQC equations can be naturally identified with their initial data at the bounce surface. It turns out that the qualitative features of the relevant dynamical evolution are largely dictated by the ratio of the kinetic to the potential energy in this initial data. In particular, as we will see in section IV C, only those dynamical trajectories for which the kinetic energy overwhelmingly dominates fail to lie in  $R(E)$ . To bring out this point, in section IV B we will study in detail the solutions in which the kinetic energy completely overwhelms the potential energy at the bounce. In section IV C we first briefly discuss dynamics in other solutions and then show that except in the case of *very extreme* kinetic energy domination at the bounce, the solutions necessarily lie in  $R(E)$ . In section IV D we find a bound on the relative volume of  $R(E)$  which shows that the probability of seeing the desired phase of slow roll inflation is extremely close to 1 in LQC. While the detailed discussion uses a quadratic potential, we argue that the qualitative result is likely to hold much more generally.

##### A. The desired slow roll

Let us begin by recalling the slow roll parameters that are used in the discussion of the WMAP data. There are two conceptually distinct sets of parameters [33]

$$\epsilon = -\frac{\dot{H}}{H^2}, \quad \eta = \frac{\ddot{H}}{\dot{H}H} \quad \text{and} \quad \epsilon_V := \frac{1}{16\pi} \left(\frac{V'}{V}\right)^2 m_{\text{Pl}}^2, \quad \eta_V = \frac{V''}{8\pi V} m_{\text{Pl}}^2. \quad (4.1)$$

Smallness of the first set ensures that the Hubble parameter is changing very slowly in the dynamical phase under consideration. (Sometimes one uses the symbol  $\epsilon_H$  for  $\epsilon$  and  $\eta_H$  for  $\eta$  to highlight this.) Inflation —i.e., accelerated expansion— is characterized by  $\epsilon < 1$ . For slow roll, on the other hand, we need  $\epsilon \ll 1$  and  $\eta \ll 1$ . As is common in the literature, in our study of slow roll, we will keep terms of order 1 in these parameters but ignore higher order terms. For concreteness, we will end the slow roll phase when  $\epsilon = 0.1$  so that the errors will be less than a percent. In theoretical investigations one often uses the second set of slow roll parameters which is tailored to the properties of the potential. During the epoch in which general relativity is an excellent approximation, the two sets are closely related by dynamics. In particular,  $\epsilon_V = [(1 + \eta/3)/(1 - \epsilon/3)]^2 \epsilon$ . Hence the difference between  $\epsilon$  and  $\epsilon_V$  is of second order in  $\epsilon, \eta$ . Finally, these parameters are best suited for studying dynamics during the general relativity era. In full LQC, on the other hand,  $\dot{H} = 0$  at the end of super-inflation but the super-inflation phase is far from being quiescent if the bounce is kinetic energy dominated. A better definition of the first slow roll parameter is  $\epsilon = (3KE)/(2\rho)$ . In general relativity, this definition agrees with (4.1) but with this definition the slow roll condition  $\epsilon \ll 1$  is violated even at the end of super-inflation if the bounce is kinetic energy dominated. In this paper we will use the standard definition (4.1) because all our slow roll considerations will refer only to the general relativity epoch.

Next, let us recall the constraints imposed by the WMAP data on scalar perturbations. The data is tailored to the co-moving wave number  $k_*$  given by [6]

$$\frac{k_*}{a_o} = 2 \times 10^{-3} \text{ Mpc}^{-1} \quad \text{or} \quad k_* = 8.58 k_o \quad (4.2)$$

where  $a_o$  refers to the scale factor today and, as before,  $k_o$  refers to the wave number that has just re-entered the Hubble radius today. (It is only the combination  $k_*/a_o$  that has direct physical meaning;  $2\pi a_o/k_o$  is the physical wave length of this reference mode today.) Within inflationary models, the data constrains initial values of fields describing the homogeneous isotropic background at time  $t(k_*)$  i.e., *the time at which the mode  $k_*$  exits the Hubble radius during inflation*. In the rest of this subsection, we will make these constraints explicit.

The amplitude  $A(t(k_*))$  of the scalar power spectrum  $\Delta_R^2(k_*)$  at this wave number is given by:

$$A(t(k_*)) = \frac{H^2(t(k_*))}{\pi \epsilon(t(k_*)) m_{\text{Pl}}^2} = 2.43 \times 10^{-9} \quad (4.3)$$

and the scalar spectral index  $n_S(k_*)$  is given by

$$n_s(t(k_*)) = 1 - \left. \frac{d \ln \Delta_R^2}{d \ln k} \right|_{k_*} = 0.968 \quad (4.4)$$

with error bars of about  $\pm 4.50\%$  for  $A$  and  $\pm 1.25\%$  for  $n_S$  [6].

In the next two sub-sections, we will focus on the quadratic potential,  $V(\phi) = (1/2)m^2\phi^2$ . The equation of motion of the scalar field (2.5) then simplifies to:

$$\ddot{\phi} + 3H\dot{\phi} + m^2\phi = 0. \quad (4.5)$$

For this potential,  $1 - n_S = 4\epsilon$  (irrespective of the value of the inflaton mass) so we conclude that the value of the slow roll parameter at the time  $t(k_*)$  is given by:

$$\epsilon(t(k_*)) = 8 \times 10^{-3}. \quad (4.6)$$

The observed value of the amplitude of the scalar power spectrum then determines the Hubble parameter  $H(t(k_\star))$  and the Hubble radius  $R_H(t(k_\star))$ :

$$H(t(k_\star)) = 7.83 \times 10^{-6} m_{\text{Pl}} \quad \text{or} \quad R_H(t(k_\star)) = 1.28 \times 10^5 \ell_{\text{Pl}} \quad (4.7)$$

Therefore, it follows from our discussion in section II A that *the LQC corrections to general relativity are highly suppressed at  $t = t(k_\star)$  and thereafter*. For simplicity, we will use this fact in what follows.

Using the approximation  $\epsilon = \epsilon_V$  at time  $t(k_\star)$  (which is consistent with observational error bars) we can determine  $\phi(t(k_\star))$  from (4.6). Then, using the implication  $\epsilon/3 = \dot{\phi}^2/(\dot{\phi}^2 + m^2\phi^2)$  of the definition of  $\epsilon$ , and the Friedmann equation, it is easy to obtain the following values

$$\begin{aligned} \phi(t(k_\star)) &= \pm 3.15 m_{\text{Pl}}, & \dot{\phi}(t(k_\star)) &= \mp 1.98 \times 10^{-7} m_{\text{Pl}}^2 \\ m &= 1.21 \times 10^{-6} m_{\text{Pl}} & \eta(t(k_\star)) &= 1.61 \times 10^{-2}. \end{aligned} \quad (4.8)$$

(In the reduced Planck units, often used in the cosmological literature, the inflaton mass is  $m = 6.06 \times 10^{-6} M_{\text{Pl}}$ .) Because this value of  $m$  is somewhat different from that given in [16], which was used in [5], some of the details of numerical results in this section differ from those reported there. However, as noted in [5], the main results reported there do not change appreciably even if this value is changed by a couple of orders of magnitude.

For the desired slow roll, without loss of generality we can assume  $\phi(t(k_\star)) < 0$  and  $(\dot{\phi})(t(k_\star)) > 0$ , so that  $\phi$  decreases as the inflaton slides down the potential. Then we can ask for the number of e-foldings of slow roll inflation starting from this time,  $t = t(k_\star)$  when  $\epsilon = 8 \times 10^{-3}$  until it increases to 0.1. *This is the ‘desired’ slow roll phase of interest to our analysis.* We have:

$$\begin{aligned} \mathcal{N} &:= \ln \frac{a_{\text{end}}}{a(t(k_\star))} = \int_{\phi(t(k_\star))}^{\phi_{\text{end}}} \frac{H}{\dot{\phi}} d\phi = -\frac{8\pi}{m_{\text{Pl}}^2} \int_{\phi(t(k_\star))}^{\phi_{\text{end}}} \frac{(1 + \frac{\eta}{3})}{(1 - \frac{\epsilon}{3})} \frac{V}{V'} d\phi \\ &\approx \frac{2\pi}{m_{\text{Pl}}^2} \left[ \left(1 + \frac{\eta}{3}\right) \left(1 + \frac{\epsilon}{3}\right) \phi^2 \right]_{\text{end}}^{t(k_\star)} \approx \frac{2\pi}{m_{\text{Pl}}^2} [\phi^2(t(k_\star)) - \phi_{\text{end}}^2] \approx 57.5 \end{aligned} \quad (4.9)$$

where in the second line we have ignored second and higher order terms in the slow roll parameters.<sup>6</sup> For simplicity, here we have used the general relativity field equations. The LQC result

$$\mathcal{N} = \frac{2\pi}{m_{\text{Pl}}^2} \left[ \left(1 + \frac{\eta}{3}\right) \left(1 + \frac{\epsilon}{3}\right) \phi^2 \left[ 1 - \frac{V(\phi)}{2(1 - \frac{\epsilon}{3})\rho_{\text{crit}}} \right] \right]_{\text{end}}^{t(k_\star)} \quad (4.10)$$

gives corrections of order  $(\phi/\phi_{\text{max}})^2 \sim 10^{-10}$  which are totally negligible.

---

<sup>6</sup> Consistency with assumptions made in the inflationary scenario require the actual slow roll to begin somewhat earlier because  $k_\star = 8.58k_o$  and the use of Bunch-Davis vacuum requires the mode  $k_o$  to be well within the Hubble radius at the onset. The initial data we begin with ensures that this will be the case. If we assume that at the onset the  $R_H$  is 100 times the physical wavelength of the mode  $k_o$ , then there are  $\sim 6.75$  e-foldings between the onset and  $t(k_\star)$ , bringing the total number of slow roll e-foldings from the onset until the end (i.e. until  $\epsilon = 0.1$ ) to  $\mathcal{N}_{\text{total}} \sim 64$ . This is a lower bound; an earlier onset and hence a larger number of e-foldings is permissible within this scenario.

To summarize, assuming the inflationary scenario with a quadratic potential, the WMAP data provides us within observational errors of  $\lesssim 2\%$ : i) the value of the inflaton mass; and ii) the initial data for inflation at some time  $t(k_*)$  in the early history of the universe. This data then automatically leads to the desired slow roll inflation with  $\sim 57$  e-foldings starting  $t = t(k_*)$ . The question now is: What is the probability that the LQC dynamical trajectories pass through this very small region of the phase space, *irrespective of what their initial data are at the bounce surface?*

## B. Extreme kinetic energy domination at the bounce

In this sub-section we will study in detail the LQC dynamics of solutions for which less than  $10^{-10}$  of energy density is in the potential at the bounce. Recall that, since the total matter density at the bounce always equals  $\rho_{\text{crit}}$ , the value  $|\phi_B|$  of the scalar field at the bounce point is bounded above by  $\phi_{\text{max}} = 0.90 m_{\text{Pl}}^2/m \approx 7.47 \times 10^5 m_{\text{Pl}}$ . We will use the fraction

$$f := \frac{\phi_B}{\phi_{\text{max}}} \quad (4.11)$$

to bin the solutions. By definition,  $f$  takes values in the interval  $[-1, 1]$ . Note also that  $f^2 = V(\phi)/\rho_{\text{crit}}$ , the fraction of the total energy density at the bounce that is in the potential. Therefore in this section we will focus on solutions with  $|f| < 10^{-5}$ . Starting at the bounce, we will first describe the main features of the LQC evolution using suitable analytical approximations and compare these with results obtained by numerical evolution of the exact system.

Let us begin by noting a symmetry of the phase space equations of motion: Given a solution  $(\phi(t), p_\phi(t); v(t), b(t))$  to (2.8) and (2.9),  $(-\phi(t), -p_\phi(t); v(t), b(t))$  is also a solution. Therefore, in the discussion of dynamics it suffices to focus on the initial data at the bounce point where  $p_\phi|_B \geq 0$ , i.e.,  $\dot{\phi}_B \geq 0$ , allowing  $\phi_B$  to take both positive and negative values. The numerical simulations were performed in these two sectors. The analytical considerations presented in this section are meant to provide a physical understanding of the main features of the early phases of LQC dynamics. Since these do not depend on the sign of  $\phi_B$ , for concreteness, in the detailed discussion of analytical considerations we will assume  $\phi_B$  to be non-negative (which corresponds to numerical simulations reported in Table I) and comment on the  $\phi_B < 0$  case only at the end.

### 1. Super-inflation

Immediately after the bounce, there is a super-inflation phase. Since the potential energy at the bounce is very low, this phase of evolution can be well approximated by adding only small corrections to the analytically well-understood massless case [12, 15]. From the bounce to the end of super-inflation, the pair  $(H, \dot{H})$  goes from  $(H = 0, \dot{H} = 10.28(1 - f^2))$  to  $(H = 0.93, \dot{H} = 0)$  in Planck units. Thus, this phase is *highly* dynamical for the Hubble parameter. Let us ignore terms of the order  $f^4$ . Then, the amount of time,  $\Delta t$ , that super-inflation lasts is well approximated by

$$\Delta t \approx \frac{\Delta H}{\dot{H}_{\text{avg}}} \approx \frac{H_{\text{max}}}{2\pi\dot{\phi}_B^2} = \frac{H_{\text{max}}}{4\pi\rho_{\text{crit}}(1 - f^2)} \approx \frac{H_{\text{max}}}{4\pi\rho_{\text{crit}}} (1 + f^2) \approx 0.18 s_{\text{Pl}} \quad (4.12)$$



How much does the volume change? We can estimate the number of e-foldings from the bounce to the end of super-inflation as follows:

$$\log(N) = \int H dt \approx H_{\text{avg}} \Delta t \approx \frac{H_{\text{max}}^2}{8\pi\rho_{\text{crit}}} (1 + f^2) \quad (4.13)$$

This implies that the number of e-foldings during super-inflation is only about 1.09. During this time the change in the value of the inflaton is given by:

$$\Delta\phi = \int \dot{\phi} dt \approx \dot{\phi}_{\text{avg}} \Delta t \approx \frac{1.41 H_{\text{max}}}{8\pi\sqrt{\rho_{\text{crit}}}} \left(1 - \frac{f^4}{2}\right) \approx 0.14 \left(1 - \frac{f^4}{2}\right) m_{\text{Pl}} \quad (4.14)$$

which is also very small. Thus, although the change in the value of the Hubble parameter during super-inflation is dramatic, because the duration of this phase is so short, the total changes in the values of the scale factor and the inflaton are also very small. While we approximated  $\dot{H}$  and  $\dot{\phi}$  by their average values in these calculations, the final results for  $\Delta t$  and  $\Delta\phi$  are in excellent agreement with the exact numerical calculations summarized in Table I.

*Remark:* Dynamics during inflation is often described using an analogy with a damped simple harmonic oscillator. This is because when the slow roll conditions hold  $H$  is approximately constant and equation (4.5) resembles that satisfied by a damped harmonic oscillator, with damping parameter  $\zeta = 3H/2m$ . Although the universe does undergo an accelerated expansion during super-inflation, since  $H$  changes radically, intuition derived from a damped harmonic oscillator is not useful in this phase. At the end of super-inflation, the Hubble parameter takes its maximum value,  $H_{\text{max}} = 0.93 m_{\text{Pl}}$ . Therefore, the ‘friction term’  $\zeta = 3H/2m$  is extremely large,  $\zeta \sim 1.15 \times 10^6$ . However, because the kinetic energy is very large—approximately half that at the bounce—it still takes an appreciable time for the inflaton to slow down. During this rather long period, dynamics is still not mimicked by a damped harmonic oscillator. It is only when the potential energy dominates—as is the case during the desired slow roll—that the analogy becomes useful.

## 2. From the end of super-inflation to turn around

Let us now consider the post-super-inflation phase. An analytical calculation can be carried out in two steps with approximations tailored to each case: i) the phase which commences at the end of super-inflation and ends when the kinetic energy equals the potential energy; and ii) the phase between the time this equality is reached and turn-around of the inflaton, i.e., when the kinetic energy reduces to zero. Dynamics has qualitatively different features in these two phases because the first is dominated by kinetic energy and the second by potential.

In phase i), the ratio of the potential to the kinetic energy is function  $\alpha(t)$  which takes values in  $(0, 1)$ . The approximation consists of replacing it with its ‘average’ value  $\alpha_o$ . At the end of the calculation,  $\alpha_o$  is determined by comparing the analytic expression with the exact numerical answer in one of the cases given in Table I and then used in other cases. We start with the equation  $\dot{b} = -4\pi\gamma\dot{\phi}^2$  from (2.9) and, using the constraint equation (2.8) and the approximation, obtain a differential equation containing only  $b$ . The solution  $b(t)$  is given by

$$\cot \lambda b(t) - \cot \lambda b(t_e) = \frac{2.4439 \lambda (t - t_e)}{1 + \alpha_o} \quad (4.15)$$

| $f$                   | Event                         | $\phi$                | $\dot{\phi}$           | $H$                   | $\dot{H}$               | $t$                   | $\epsilon$         |
|-----------------------|-------------------------------|-----------------------|------------------------|-----------------------|-------------------------|-----------------------|--------------------|
| $1.07 \times 10^{-6}$ | Bounce                        | $8.00 \times 10^{-1}$ | $9.05 \times 10^{-1}$  | <b>0</b>              | $1.03 \times 10^1$      | <b>0</b>              | $\infty$           |
|                       | End of SI                     | $9.44 \times 10^{-1}$ | $6.39 \times 10^{-1}$  | $9.26 \times 10^{-1}$ | <b>0</b>                | $1.80 \times 10^{-1}$ | <b>0</b>           |
|                       | $KE = PE$                     | 2.91                  | $3.52 \times 10^{-6}$  | $1.02 \times 10^{-5}$ | $-1.56 \times 10^{-10}$ | $4.04 \times 10^4$    | 1.50               |
|                       | $\dot{\phi} = 0$              | 3.03                  | <b>0</b>               | $7.50 \times 10^{-6}$ | <b>0</b>                | $1.66 \times 10^5$    | <b>0</b>           |
|                       | $\epsilon = 8 \times 10^{-3}$ | 3.01                  | $-1.88 \times 10^{-7}$ | $7.46 \times 10^{-6}$ | $-4.45 \times 10^{-13}$ | $3.05 \times 10^5$    | $8 \times 10^{-3}$ |
| $1.17 \times 10^{-6}$ | Bounce                        | $8.75 \times 10^{-1}$ | $9.05 \times 10^{-1}$  | <b>0</b>              | $1.03 \times 10^1$      | <b>0</b>              | $\infty$           |
|                       | End of SI                     | 1.02                  | $6.39 \times 10^{-1}$  | $9.26 \times 10^{-1}$ | <b>0</b>                | $1.80 \times 10^{-1}$ | <b>0</b>           |
|                       | $KE = PE$                     | 2.98                  | $3.61 \times 10^{-6}$  | $1.04 \times 10^{-5}$ | $-1.63 \times 10^{-10}$ | $3.94 \times 10^4$    | 1.50               |
|                       | $\dot{\phi} = 0$              | 3.10                  | <b>0</b>               | $7.67 \times 10^{-6}$ | <b>0</b>                | $1.63 \times 10^5$    | <b>0</b>           |
|                       | $\epsilon = 8 \times 10^{-3}$ | 3.07                  | $1.92 \times 10^{-7}$  | $7.62 \times 10^{-6}$ | $-4.56 \times 10^{-13}$ | $3.28 \times 10^5$    | $8 \times 10^{-3}$ |
| $1.25 \times 10^{-6}$ | Bounce                        | $9.37 \times 10^{-1}$ | $9.05 \times 10^{-1}$  | <b>0</b>              | $1.03 \times 10^1$      | <b>0</b>              | $\infty$           |
|                       | End of SI                     | 1.08                  | $6.39 \times 10^{-1}$  | $9.26 \times 10^{-1}$ | <b>0</b>                | $1.80 \times 10^{-1}$ | <b>0</b>           |
|                       | $KE = PE$                     | 3.04                  | $3.67 \times 10^{-6}$  | $1.06 \times 10^{-5}$ | $-1.69 \times 10^{-10}$ | $3.87 \times 10^4$    | 1.50               |
|                       | $\dot{\phi} = 0$              | 3.16                  | <b>0</b>               | $7.82 \times 10^{-6}$ | <b>0</b>                | $1.60 \times 10^5$    | <b>0</b>           |
|                       | $\epsilon = 8 \times 10^{-3}$ | 3.12                  | $-1.95 \times 10^{-7}$ | $7.75 \times 10^{-6}$ | $-4.81 \times 10^{-13}$ | $3.75 \times 10^5$    | $8 \times 10^{-3}$ |
| $1.42 \times 10^{-6}$ | Bounce                        | 1.06                  | $9.05 \times 10^{-1}$  | <b>0</b>              | $1.03 \times 10^1$      | <b>0</b>              | $\infty$           |
|                       | End of SI                     | 1.20                  | $6.39 \times 10^{-1}$  | $9.26 \times 10^{-1}$ | <b>0</b>                | $1.80 \times 10^{-1}$ | <b>0</b>           |
|                       | $KE = PE$                     | 3.16                  | $3.81 \times 10^{-6}$  | $1.10 \times 10^{-5}$ | $-1.82 \times 10^{-10}$ | $3.73 \times 10^4$    | 1.50               |
|                       | $\dot{\phi} = 0$              | 3.28                  | <b>0</b>               | $8.11 \times 10^{-6}$ | <b>0</b>                | $1.56 \times 10^5$    | <b>0</b>           |
|                       | $\epsilon = 8 \times 10^{-3}$ | 3.15                  | $-1.97 \times 10^{-7}$ | $7.82 \times 10^{-6}$ | $-4.86 \times 10^{-13}$ | $8.23 \times 10^5$    | $8 \times 10^{-3}$ |
| $1.59 \times 10^{-6}$ | Bounce                        | 1.19                  | $9.05 \times 10^{-1}$  | <b>0</b>              | $1.03 \times 10^1$      | <b>0</b>              | $\infty$           |
|                       | End of SI                     | 1.33                  | $6.39 \times 10^{-1}$  | $9.26 \times 10^{-1}$ | <b>0</b>                | $1.80 \times 10^{-1}$ | <b>0</b>           |
|                       | $KE = PE$                     | 3.28                  | $3.96 \times 10^{-6}$  | $1.15 \times 10^{-5}$ | $-1.97 \times 10^{-10}$ | $3.59 \times 10^4$    | 1.50               |
|                       | $\dot{\phi} = 0$              | 3.40                  | <b>0</b>               | $8.42 \times 10^{-6}$ | <b>0</b>                | $1.51 \times 10^5$    | <b>0</b>           |
|                       | $\epsilon = 8 \times 10^{-3}$ | 3.15                  | $-1.97 \times 10^{-7}$ | $7.82 \times 10^{-6}$ | $-4.87 \times 10^{-13}$ | $1.45 \times 10^6$    | $8 \times 10^{-3}$ |
| $1.77 \times 10^{-6}$ | Bounce                        | 1.32                  | $9.05 \times 10^{-1}$  | <b>0</b>              | $1.03 \times 10^1$      | <b>0</b>              | $\infty$           |
|                       | End of SI                     | 1.46                  | $6.39 \times 10^{-1}$  | $9.26 \times 10^{-1}$ | <b>0</b>                | $1.80 \times 10^{-1}$ | <b>0</b>           |
|                       | $KE = PE$                     | 3.40                  | $4.11 \times 10^{-6}$  | $1.19 \times 10^{-5}$ | $-2.13 \times 10^{-10}$ | $3.46 \times 10^4$    | 1.50               |
|                       | $\dot{\phi} = 0$              | 3.52                  | <b>0</b>               | $8.73 \times 10^{-6}$ | <b>0</b>                | $1.47 \times 10^5$    | <b>0</b>           |
|                       | $\epsilon = 8 \times 10^{-3}$ | 3.15                  | $-1.97 \times 10^{-7}$ | $7.82 \times 10^{-6}$ | $-4.87 \times 10^{-13}$ | $2.08 \times 10^6$    | $8 \times 10^{-3}$ |

TABLE I: Dynamical evolution of  $\phi$  and  $H$  for various values of  $f$  in the case  $\phi_B > 0$ . Analytical considerations imply that certain entries should be identically zero; their values are  $O(\epsilon_{machine})$  in simulations but denoted by a boldface zero (**0**) in the Table. Events considered are: the bounce point, end of super-inflation (End of SI), equality of potential and kinetic energy ( $KE = PE$ ), turn around ( $\dot{\phi} = 0$ ), and reaching  $\epsilon = 8 \times 10^{-3}$ . The desired slow roll compatible with the WMAP data is not realized if  $f \leq 1.17 \times 10^{-6}$  but is realized for  $f \geq 1.25 \times 10^{-6}$ .

where  $t_e$  is the proper time at the end of super-inflation. It can be substituted back in the original Friedmann equation to obtain  $t - t_e$  as a function of  $\phi(t) - \phi(t_e)$ . Finally, we set

| Method            | $\phi_e = 9.44 \times 10^{-1}$ | $\phi_e = 1.02$    | $\phi_e = 1.08$    | $\phi_e = 1.20$    | $\phi_e = 1.33$    | $\phi_e = 1.46$    |
|-------------------|--------------------------------|--------------------|--------------------|--------------------|--------------------|--------------------|
| Exact Numerics    | $4.04 \times 10^4$             | $3.94 \times 10^4$ | $3.87 \times 10^4$ | $3.73 \times 10^4$ | $3.59 \times 10^4$ | $3.46 \times 10^4$ |
| Analytic Eq(4.17) | $4.00 \times 10^4$             | $3.91 \times 10^4$ | $3.84 \times 10^4$ | $3.71 \times 10^4$ | $3.58 \times 10^4$ | $3.46 \times 10^4$ |

TABLE II: The time interval  $t_{\text{Eq}} - t_e$  as a function of the value  $\phi_e$  of in the inflaton at the end of super-inflation: Comparison between the exact numerical result and the analytical approximation. As  $\phi_e$  increases, the difference between kinetic and potential energies at the end of super-inflation decreases, whence it less takes less time to achieve equality between potential and kinetic energy. The analytical approximation replaced the ratio  $\alpha(t)$  between the two energies by an ‘average’  $\alpha_o$  during this phase i) after the end of super-inflation.

$t = t_{\text{Eq}}$ , the time at which kinetic and potential energies are equal, to obtain:

$$\phi(t_{\text{Eq}}) - \phi(t_e) = 0.1628 \sqrt{1 + \alpha_o} (y_{\text{Eq}} - y_e) \quad \text{where} \quad \sinh(y) = 1 + \left(\frac{5.56}{1 + \alpha_o}\right)t. \quad (4.16)$$

Next, the constraint equation (2.8) determines  $\phi(t_{\text{Eq}})$  in terms of  $b(t_{\text{Eq}})$  and we can invert the expression (4.15) of  $b(t)$  to eliminate it in favor of  $t_{\text{Eq}} - t_e$ . The result is an expression relating  $t_{\text{Eq}} - t_e$  and  $\phi(t_e)$  alone. It determines how long the first post-super-inflation phase lasts for any given value  $\phi_e$  of the inflaton at the end of super-inflation:

$$\begin{aligned} \phi_e &= \frac{1}{m} \frac{0.640}{\sqrt{1 + \left(1 + \frac{5.56}{1 + \alpha_o} (t_{\text{Eq}} - t_e)\right)^2}} - 0.1628 \sqrt{1 + \alpha_o} (y_{\text{Eq}} - y_e) \\ &\approx \frac{9.508 \times 10^4 (1 + \alpha_o)}{t_{\text{Eq}}} - 0.1628 \sqrt{1 + \alpha_o} \left( \sinh^{-1} \left(1 + \frac{5.56(t_{\text{Eq}})}{1 + \alpha_o}\right) - 0.88 \right) \end{aligned} \quad (4.17)$$

where for simplicity we set  $t_e = 0$  in the last step. Comparison of this expression with the entry  $f = 1.77 \times 10^{-6}$  in table Table I, one finds that the fit with the exact numerical result is best when  $\alpha_o = 1/3$ . We will use this value and compare the approximate analytical expression with the exact numerical result in all cases covered in Table I. The resulting Table II shows that the agreement is very good; the analytical approximation we made by replacing  $\alpha$  with its ‘average’  $\alpha_o$  works quite well. Table II also shows that the duration  $t_{\text{Eq}} - t_e \sim 10^4 s_{\text{Pl}}$  of phase i) is *much* longer than that of super-inflation.

Eq (4.17) determines the duration  $t_{\text{Eq}} - t_e$  of phase i) as a function of the value of the inflation at the end of super-inflation. The same approximation as was used there provides expressions for values of  $H, \phi, \dot{\phi}$  at the end of phase i) as a function of  $t_{\text{Eq}} - t_e$ :

$$H(t_{\text{Eq}}) \approx \frac{1 + \alpha_o}{3.00(t_{\text{Eq}} - t_e)}; \quad \dot{\phi}(t_{\text{Eq}}) \approx \frac{0.1152(1 + \alpha_o)}{t_{\text{Eq}} - t_e}; \quad \phi(t_{\text{Eq}}) \approx \frac{9.5207 \times 10^4 (1 + \alpha_o)}{t_{\text{Eq}} - t_e}. \quad (4.18)$$

Again, there is good agreement with the exact numerical results. For the Hubble parameter a comparison is given in Table III.

Thus the analytic approximation yields a good portrait of dynamics of all physical quantities of interest. Note that the Hubble parameter changes very significantly during this phase also: At the end of super-inflation, we have  $H \approx 0.93 m_{\text{Pl}}$  while at  $t_{\text{Eq}}$ ,  $H \approx 10^{-5} m_{\text{Pl}}$ . Similarly, while  $\dot{\phi} \approx 0.9 m_{\text{Pl}}^2$  at the end of super-inflation, we have  $\dot{\phi}(t_{\text{Eq}}) \approx 4 \times 10^{-6} m_{\text{Pl}}^2$ .

| Method            | $\phi_e = 9.44 \times 10^{-1}$ | $\phi_e = 1.02$       | $\phi_e = 1.08$       | $\phi_e = 1.20$       | $\phi_e = 1.33$       | $\phi_e = 1.46$       |
|-------------------|--------------------------------|-----------------------|-----------------------|-----------------------|-----------------------|-----------------------|
| Exact Numerics    | $1.02 \times 10^{-5}$          | $1.04 \times 10^{-5}$ | $1.06 \times 10^{-5}$ | $1.10 \times 10^{-5}$ | $1.15 \times 10^{-5}$ | $1.19 \times 10^{-5}$ |
| Analytic Eq(4.18) | $1.11 \times 10^{-5}$          | $1.13 \times 10^{-5}$ | $1.15 \times 10^{-5}$ | $1.19 \times 10^{-5}$ | $1.24 \times 10^{-5}$ | $1.28 \times 10^{-5}$ |

TABLE III: Value of the Hubble parameter  $H$  at  $t = t_{\text{Eq}}$  as a function of the value  $\phi_e$ : Comparison between the exact numerical result and the analytical approximation. The analytical approximation replaced the ratio  $\alpha(t)$  between the two energies by an ‘average’  $\alpha_o$  during this phase i) after the end of super-inflation. The resulting error is less than 10%. Since  $\phi_e \approx \phi_B = f\phi_{\text{max}}$ ,  $H(t_{\text{Eq}})$  increases monotonically with  $f$ . Since  $H(t_{\text{Eq}}) \approx 10^{-5}m_{\text{Pl}}$ , general relativity is an excellent approximation to LQC at  $t = t_{\text{Eq}}$ .

| Method            | $\phi_e = 9.44 \times 10^{-1}$ | $\phi_e = 1.02$    | $\phi_e = 1.08$    | $\phi_e = 1.20$    | $\phi_e = 1.33$    | $\phi_e = 1.46$    |
|-------------------|--------------------------------|--------------------|--------------------|--------------------|--------------------|--------------------|
| Exact Numerics    | $1.26 \times 10^5$             | $1.24 \times 10^5$ | $1.21 \times 10^5$ | $1.19 \times 10^5$ | $1.15 \times 10^5$ | $1.12 \times 10^5$ |
| Analytic Eq(4.18) | $1.26 \times 10^5$             | $1.23 \times 10^5$ | $1.21 \times 10^5$ | $1.17 \times 10^5$ | $1.12 \times 10^5$ | $1.08 \times 10^5$ |

TABLE IV: Duration of phase ii),  $t_{\text{TA}} - t_{\text{Eq}}$ , as a function of  $\phi_e$ : Comparison between the exact numerical result and the analytical approximation. The analytical approximation assumes that  $\ddot{\phi}_{\text{Avg}}$  is given by  $\beta \times \ddot{\phi}(t_{\text{Eq}})$  where  $\beta$  is set equal to 1/4 by agreement with numerical values for  $\phi_e = 0.944m_{\text{Pl}}$ . the analytical expression then reproduces the exact numerical results for other values of  $\phi_e$  to within 4%.

Let us now turn to the subsequent phase ii) which lasts until the inflaton turns around, i.e., its kinetic energy vanishes identically. Since the energy density has dramatically decreased during phase i) —at  $t_{\text{Eq}}$ , the matter density  $\rho(t_{\text{Eq}})$  is of the order  $10^{-11}\rho_{\text{Pl}}$  in all cases given in Table III— general relativity is an excellent approximation in this phase. Also, since the kinetic energy is sub-dominant, in contrast to phase i), phase ii) is dynamically rather quiescent. At the start of this phase, values of  $H, \phi, \dot{\phi}$  are given by (4.18). Using them and (4.5) we can calculate  $\ddot{\phi}(t_{\text{Eq}})$  and  $\ddot{\phi}(t_{\text{Eq}})$ . In all cases summarized in Table III,  $\ddot{\phi}(t_{\text{Eq}}) \sim 10^{-10}m_{\text{Pl}}^2$  and  $\ddot{\phi}(t_{\text{Eq}}) \lesssim 10^{-16}m_{\text{Pl}}^3$ . Because of this quiescent behavior we can hope to obtain the time duration  $(t_{\text{TA}} - t_{\text{Eq}})$  until the turn around by a simple calculation:

$$\begin{aligned}
(t_{\text{TA}} - t_{\text{Eq}}) &\approx \frac{\Delta\dot{\phi}}{\ddot{\phi}_{\text{avg}}} \approx -\frac{\dot{\phi}(t_{\text{Eq}})}{\beta\ddot{\phi}(t_{\text{Eq}})} \\
&\approx \frac{\dot{\phi}(t_{\text{Eq}})}{\beta(3H(t_{\text{Eq}}) + m)\dot{\phi}(t_{\text{Eq}})} = \frac{1}{\beta(3H(t_{\text{Eq}}) + m)}
\end{aligned} \tag{4.19}$$

where  $\beta$  is a coefficient (of  $O(1)$ ) relating the value of  $\ddot{\phi}$  at  $t = t_{\text{Eq}}$  to its average value in phase ii). (As explained in the caption of Table IV,  $\beta$  was set to 1/4 in numerical evaluations of (4.19).)

Table IV provides a comparison with the exact numerical values and those calculated using (4.19). Note that the quiescent phase ii) lasts even longer than the more dynamic phase i). In the case of super-inflation we could use the ‘averaging approximation’ because, although the Hubble parameter is very dynamic, the phase is very short lived. In phase ii) we could use it because although the phase is long lived, it is quiescent. Finally, although phase ii) lasts  $\sim 10^5 s_{\text{Pl}}$ , because  $\dot{H}, \dot{\phi}$  are  $\lesssim 10^{-10}, \lesssim 10^{-6}$  at  $t = t_{\text{Eq}}$ , the change in  $H, \phi$

during phase ii) is quite small, again highlighting the quiescent nature of the phase.

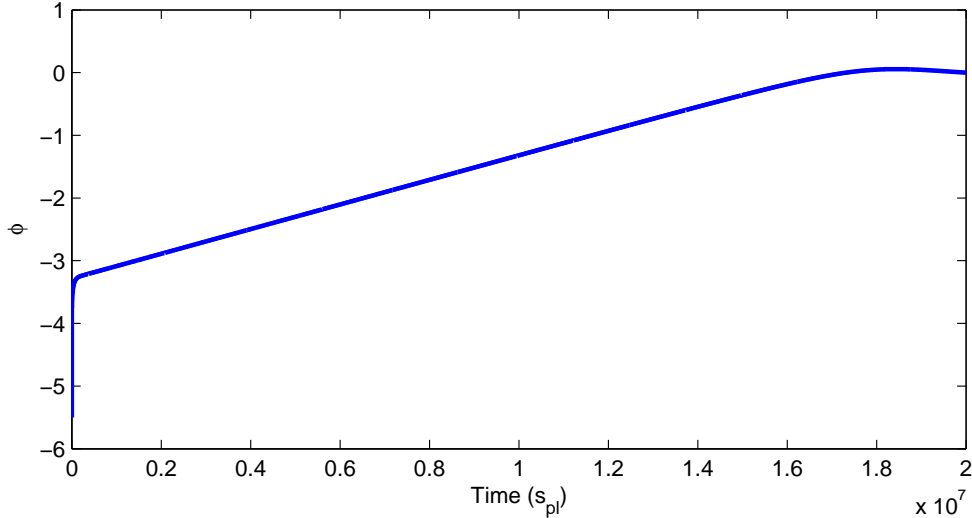


FIG. 1: Illustrative evolution of the scalar field. In this plot we use a negative value of  $\phi_B$  to complement the analytical discussion:  $\phi_B = -5.5 m_{\text{Pl}}$  and  $\dot{\phi}_B > 0$ . (See the case  $f = -7.35 \times 10^{-6}$  in Table V.) The inflaton rolls down the potential quickly at first because the kinetic energy at the bounce is large. The kinetic energy equals potential energy at  $t = t_{\text{Eq}} \equiv 3.51 \times 10^4 s_{\text{Pl}}$  and  $\phi$  changes more slowly during the subsequent quiescent phase. The WMAP value  $\epsilon = 8 \times 10^{-3}$  is reached  $t = 7.08 \times 10^5 s_{\text{Pl}}$  and the end of slow roll,  $\epsilon = 0.1$ , used in this paper is reached at  $t = 1.24 \times 10^7 s_{\text{Pl}}$ . Because  $\phi_B$  is negative, in this case the inflaton turns around after the end of the desired slow roll, at  $t = 1.84 \times 10^7 s_{\text{Pl}}$ .

### 3. Post turn-around

At the end of phase ii), the inflaton turns around and starts rolling down the potential. Since by definition  $\dot{\phi}(t_{\text{TA}}) = 0$ , the slow roll parameter  $\epsilon$  also vanishes there. However, because  $\dot{H} \propto \dot{\phi}^2$ , it also vanishes there, whence the slow roll parameter  $\eta$  need not be small and we are not assured the beginning of a slow roll. The desired slow roll, if it is realized in the given solution, must occur subsequently, as the inflaton rolls down the potential.

Recall that, for the desired slow roll to be realized, we must have  $\phi(t(k_*)) \approx 3.15 m_{\text{Pl}}$ . This point can be reached if and only if  $\phi(t_{\text{TA}}) > 3.15 m_{\text{Pl}}$ . When is this condition realized and when does it fail to be realized in the extreme kinetic energy dominated case under consideration? The analytical formulas of the last two sub-sections show that  $\phi(t_{\text{TA}})$  increases with  $f$  and the illustrative numerical values we have presented ensure that  $\phi(t_{\text{TA}}) > 3.15 m_{\text{Pl}}$  if  $\phi_B \geq 0.937 m_{\text{Pl}}$ . (This is a sufficient condition rather than a sharp bound.) Since  $|\phi| \in (0, 7.47 m_{\text{Pl}})$  in the extreme kinetic energy dominated case, our result suggests that it is likely that the desired conditions are met. However, in the analytical considerations we focused only on the  $\phi_B \geq 0$  case and moreover made some approximations. Therefore, we also carried out a large number of numerical simulations of exact equations to first confirm and then sharpen this implication. (Tables I and V contain only a few illustrative results.)

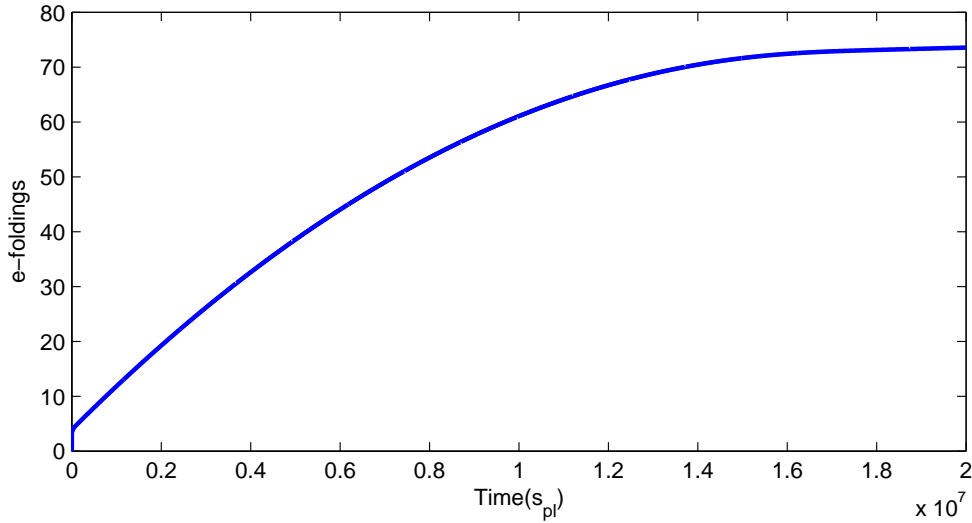


FIG. 2: Illustrative evolution of the scale factor for the same case as in Fig 1, i.e., for  $\phi_B = -5.5 m_{\text{Pl}}$  and  $\dot{\phi}_B > 0$ . (See the case  $f = -7.35 \times 10^{-6}$  in Table V.) The WMAP value  $\epsilon = 8 \times 10^{-3}$  is reached  $t = 7.08 \times 10^5 s_{\text{Pl}}$  and the end of slow roll,  $\epsilon = 0.1$ , used in this paper is reached at  $t = 1.24 \times 10^7 s_{\text{Pl}}$ . The number of e-foldings flattens out soon after this time.

The simulations were performed in MATLAB using a Runge-Kutta (4,5) ordinary differential equation solver (ODE45) with both relative and absolute tolerances set at  $3 \times 10^{-14}$ . To facilitate computation, the logarithm of the ratio of the volume at a given time to the volume at the bounce was chosen to be a fundamental variable. On each solution the preservation of the Hamiltonian constraint was verified at the level of the tolerances. For robustness sample solutions were also evolved independently with various different tolerances, using a set of equations which did not involve the initial volume, and seen to agree with those given by the Runge-Kutta algorithm. Time scales for the evolutions were chosen such that the numerical noise introduced by the deviation of the Hamiltonian constraint from zero would not contribute significantly (i.e. greater than one part in  $10^6$ ) to the fundamental variables. Separate searches were used around the end points of the allowed space, i.e., very low values of  $f$  for which the dynamical trajectories fail to be consistent with the WMAP data. This ensured that the extremely high probability we found for the LQC dynamics to be compatible with the WMAP data is in fact a lower bound.

As discussed in section IV A, for the quadratic potential the WMAP data implies that there was a time  $t(k_*)$  in the early history of the universe when  $\epsilon = 8 \times 10^{-3}$  and  $\phi = 3.15 m_{\text{Pl}}$  within error bars (of  $\lesssim 4.5\%$ ). In LQC we can specify the initial data at the bounce. Numerical simulations let us answer the following question for the extreme kinetic energy dominated bounce: What are restrictions on the initial data at the bounce for the ensuing LQC dynamical trajectory to meet the WMAP constraint? Full numerical simulations bear out conclusions suggested by Tables I and V:

$$\text{WMAP constraint is met provided } \begin{cases} f \geq 1.25 \times 10^{-6} & \text{if } \phi_B \geq 0 \\ |f| \geq 7.35 \times 10^{-6} & \text{if } \phi_B < 0 \end{cases} . \quad (4.20)$$

Thus, in the extreme kinetic dominated case, *we are guaranteed that the event  $E$  —the desired slow roll compatible with WMAP observations— will be realized in the solution under*

| $f$                    | Event                         | $\phi$                | $\dot{\phi}$          | $H$                   | $\dot{H}$               | $t$                   | $\epsilon$         |
|------------------------|-------------------------------|-----------------------|-----------------------|-----------------------|-------------------------|-----------------------|--------------------|
| $-7.02 \times 10^{-6}$ | Bounce                        | -5.25                 | $9.05 \times 10^{-1}$ | <b>0</b>              | $1.03 \times 10^1$      | <b>0</b>              | $\infty$           |
|                        | End of SI                     | -5.11                 | $6.39 \times 10^{-1}$ | $9.26 \times 10^{-1}$ | <b>0</b>                | $1.80 \times 10^{-1}$ | <b>0</b>           |
|                        | $KE = PE$                     | -3.15                 | $3.80 \times 10^{-6}$ | $1.10 \times 10^{-5}$ | $-1.82 \times 10^{-10}$ | $3.81 \times 10^4$    | 1.50               |
|                        | $\dot{\phi} = 0$              | $5.42 \times 10^{-2}$ | <b>0</b>              | $2.25 \times 10^{-7}$ | <b>0</b>                | $1.71 \times 10^7$    | <b>0</b>           |
|                        | $\epsilon = 8 \times 10^{-3}$ | NA                    | NA                    | NA                    | NA                      | NA                    | NA                 |
| $-7.22 \times 10^{-6}$ | Bounce                        | -5.40                 | $9.05 \times 10^{-1}$ | <b>0</b>              | $1.03 \times 10^1$      | <b>0</b>              | $\infty$           |
|                        | End of SI                     | -5.26                 | $6.39 \times 10^{-1}$ | $9.26 \times 10^{-1}$ | <b>0</b>                | $1.80 \times 10^{-1}$ | <b>0</b>           |
|                        | $KE = PE$                     | -3.31                 | $4.00 \times 10^{-6}$ | $1.16 \times 10^{-5}$ | $-2.01 \times 10^{-10}$ | $3.62 \times 10^4$    | 1.50               |
|                        | $\dot{\phi} = 0$              | $5.64 \times 10^{-2}$ | <b>0</b>              | $2.14 \times 10^{-7}$ | <b>0</b>                | $1.79 \times 10^7$    | <b>0</b>           |
|                        | $\epsilon = 8 \times 10^{-3}$ | NA                    | NA                    | NA                    | NA                      | NA                    | NA                 |
| $-7.35 \times 10^{-6}$ | Bounce                        | -5.50                 | $9.05 \times 10^{-1}$ | <b>0</b>              | $1.03 \times 10^1$      | <b>0</b>              | $\infty$           |
|                        | End of SI                     | -5.36                 | $6.39 \times 10^{-1}$ | $9.26 \times 10^{-1}$ | <b>0</b>                | $1.80 \times 10^{-1}$ | <b>0</b>           |
|                        | $KE = PE$                     | -3.41                 | $4.12 \times 10^{-6}$ | $1.19 \times 10^{-5}$ | $-2.14 \times 10^{-10}$ | $3.51 \times 10^4$    | 1.50               |
|                        | $\dot{\phi} = 0$              | $5.51 \times 10^{-2}$ | <b>0</b>              | $2.21 \times 10^{-7}$ | <b>0</b>                | $1.84 \times 10^7$    | <b>0</b>           |
|                        | $\epsilon = 8 \times 10^{-3}$ | -3.14                 | $1.97 \times 10^{-7}$ | $7.80 \times 10^{-6}$ | $-4.86 \times 10^{-13}$ | $7.08 \times 10^5$    | $8 \times 10^{-3}$ |
| $-7.69 \times 10^{-6}$ | Bounce                        | -5.75                 | $9.05 \times 10^{-1}$ | <b>0</b>              | $1.03 \times 10^1$      | <b>0</b>              | $\infty$           |
|                        | End of SI                     | -5.61                 | $6.39 \times 10^{-1}$ | $9.26 \times 10^{-1}$ | <b>0</b>                | $1.80 \times 10^{-1}$ | <b>0</b>           |
|                        | $KE = PE$                     | -3.68                 | $4.44 \times 10^{-6}$ | $1.29 \times 10^{-5}$ | $-2.48 \times 10^{-10}$ | $3.26 \times 10^4$    | 1.50               |
|                        | $\dot{\phi} = 0$              | $5.71 \times 10^{-2}$ | <b>0</b>              | $2.11 \times 10^{-7}$ | <b>0</b>                | $1.97 \times 10^7$    | <b>0</b>           |
|                        | $\epsilon = 8 \times 10^{-3}$ | -3.14                 | $1.97 \times 10^{-7}$ | $7.80 \times 10^{-6}$ | $-4.87 \times 10^{-13}$ | $2.03 \times 10^6$    | $8 \times 10^{-3}$ |
| $-7.92 \times 10^{-6}$ | Bounce                        | -5.92                 | $9.05 \times 10^{-1}$ | <b>0</b>              | $1.03 \times 10^1$      | <b>0</b>              | $\infty$           |
|                        | End of SI                     | -5.78                 | $6.39 \times 10^{-1}$ | $9.26 \times 10^{-1}$ | <b>0</b>                | $1.80 \times 10^{-1}$ | <b>0</b>           |
|                        | $KE = PE$                     | -3.85                 | $4.66 \times 10^{-6}$ | $1.35 \times 10^{-5}$ | $-2.73 \times 10^{-10}$ | $3.10 \times 10^4$    | 1.50               |
|                        | $\dot{\phi} = 0$              | $5.48 \times 10^{-2}$ | <b>0</b>              | $2.22 \times 10^{-7}$ | <b>0</b>                | $2.07 \times 10^7$    | <b>0</b>           |
|                        | $\epsilon = 8 \times 10^{-3}$ | -3.14                 | $1.97 \times 10^{-7}$ | $7.80 \times 10^{-6}$ | $-4.86 \times 10^{-13}$ | $2.94 \times 10^6$    | $8 \times 10^{-3}$ |
| $-8.02 \times 10^{-6}$ | Bounce                        | -6.00                 | $9.05 \times 10^{-1}$ | <b>0</b>              | $1.03 \times 10^1$      | <b>0</b>              | $\infty$           |
|                        | End of SI                     | -5.86                 | $6.39 \times 10^{-1}$ | $9.26 \times 10^{-1}$ | <b>0</b>                | $1.80 \times 10^{-1}$ | <b>0</b>           |
|                        | $KE = PE$                     | -3.94                 | $4.75 \times 10^{-6}$ | $1.38 \times 10^{-5}$ | $-2.84 \times 10^{-10}$ | $3.04 \times 10^4$    | 1.50               |
|                        | $\dot{\phi} = 0$              | $5.51 \times 10^{-2}$ | <b>0</b>              | $2.21 \times 10^{-7}$ | <b>0</b>                | $2.11 \times 10^7$    | <b>0</b>           |
|                        | $\epsilon = 8 \times 10^{-3}$ | -3.14                 | $1.97 \times 10^{-7}$ | $7.80 \times 10^{-6}$ | $-4.86 \times 10^{-13}$ | $3.36 \times 10^6$    | $8 \times 10^{-3}$ |

TABLE V: Dynamical evolution of  $\phi$  and  $H$  for various values of  $f$  in the case  $\phi_B < 0$ . Analytical considerations imply that certain entries should be identically zero; their values are  $O(\epsilon_{machine})$  in simulations but denoted by a boldface zero (**0**) in the Table. Events considered are: the bounce point, end of super-inflation (End of SI), equality of potential and kinetic energy ( $KE = PE$ ), turn around ( $\dot{\phi} = 0$ ), and reaching  $\epsilon = 8 \times 10^{-3}$ . Because  $\phi_B < 0$ , the turn around happens *after* the desired inflation ends. The desired slow roll compatible with the WMAP data is not realized if  $|f| \leq 7.22 \times 10^{-6}$  but is realized if  $|f| \geq 7.35 \times 10^{-6}$ .

consideration if  $f$  is outside the interval  $(-7.35 \times 10^{-6}, 1.25 \times 10^{-6})$ . (Again, this is only a sufficient condition.) Since full range of  $f$  in the kinetic energy dominated case under consideration is  $(-10^{-5}, 10^{-5})$ , this result suggests that  $E$  will be realized in ‘more than half the trajectories’ in this case. We will sharpen this statement using the normalized Liouville measure in section IV D.

The precise numbers in the sufficient condition (4.20) depend on the sign of  $\phi_B$  at the bounce. We will conclude with a brief discussion of the origin of the difference between the  $\phi_B > 0$  and  $\phi_B < 0$  cases. The origin of the asymmetry lies in the fact that (because of symmetries of field equations) we have restricted ourselves to data with  $\dot{\phi}_B \geq 0$ . So, if  $\phi_B < 0$ , the inflaton is already rolling down the potential at the bounce. If initially it is sufficiently high up in the potential with,  $|\phi_B| > 5.5 m_{\text{Pl}}$ , friction can slow it down sufficiently for the desired slow roll to begin at  $\phi \approx -3.15 m_{\text{Pl}}$ . But if  $|\phi_B| < 5.5 m_{\text{Pl}}$ , then the kinetic energy is too large for the friction term to slow it sufficiently for the desired slow roll to commence before it reaches the bottom of the potential. Then it starts climbing up on the  $\phi > 0$  branch but does not acquire a value higher than  $\sim 3.15$  required for the dynamical trajectory to pass through the region satisfying the WMAP constraints. In the  $\phi_B > 0$  case, by contrast, if  $\phi_B \gtrsim 0.94$ , the kinetic energy at the bounce is sufficient to propel the inflaton to values higher than  $3.15 m_{\text{Pl}}$  on the  $\phi_B > 0$  branch of the potential to allow for the desired slow roll.

In subsection IV C 2, we will show that the likelihood of attaining the desired slow roll is in fact 1 if the bounce is *not* extreme kinetic energy dominated and in section IV D we will calculate the precise probability for the occurrence of  $E$  on the entire space  $\mathbb{S}$  of solutions using the normalized Liouville measure.

### C. Generic LQC solutions and the WMAP slow roll

In section IV C 1 we continue our description of qualitative features of LQC dynamics, now for bounces with  $f > 10^{-5}$ . This discussion is rather sketchy compared to that of section IV B because in this case there are no subtleties with respect to the WMAP data: as we show in section IV C 2, all dynamical trajectories meeting this condition at the bounce satisfy the WMAP constraints.

#### 1. Evolution of other initial data: Qualitative features

We will highlight only those features which are qualitatively different from the kinetic energy dominated bounce discussed in detail in section IV B. Again, for concreteness, we will focus on the case when  $\phi_B$  and  $\dot{\phi}_B$  are both positive. Let us begin with the intermediate case  $10^{-5} < f \lesssim 1/\sqrt{2}$  where the kinetic energy still exceeds the potential energy at the bounce but does not dominate it as in section IV B. The super-inflation era is similar to that described in section IV B 1 but because  $\dot{\phi}_B$  is now lower, the phase lasts longer. The inflaton climbs up the potential but change in its value is again small. The Hubble parameter, on contrast, is again dynamical. However, the post super-inflation dynamics exhibits significant differences. For, now the value of  $\phi_B$  is higher and  $\dot{\phi}_B$  lower while, as before,  $H$  assumes its largest value at the end of super-inflation. Therefore, the coefficient of friction,  $\zeta = 3H/2m$ , is again large but there is less kinetic energy to lose before reaching the turn-around., which is now reached within  $10-100 s_{\text{Pl}}$  after the bounce. Consequently, now the change  $\phi(t_{\text{TA}}) - \phi_B$



is negligible, a key feature not shared by regime (i).

Next, let us examine the  $f \gtrsim 1/\sqrt{2}$  where the potential energy is greater than the kinetic energy. Now, the LQC effects dominate for an even longer time. Again, because  $\dot{\phi} > 0$ , the inflaton climbs up the potential but turns around earlier and earlier and the super-inflation phase lasts longer and longer as  $f$  increases. Now the turn around ( $\dot{\phi} = 0$ ) will occur *during super-inflation!* The change  $(\phi(t_{\text{TA}}) - \phi_{\text{B}})$  is even more negligible because the kinetic energy at the bounce is lower than that in the  $f < 0.5$  case. The slow roll conditions are easily met soon after turn-around. A difference from this phase of slow roll and that for  $f > 1/\sqrt{2}$  is that  $H$  continues to grow during the slow roll because we are still in the super-inflation phase. There is an enormous number of slow roll e-foldings already in the deep Planck regime where the matter density is greater than half the critical density.

## 2. Compatibility with the WMAP data

In the extreme kinetic energy domination we could carry out numerical simulations starting from the bounce until the end of the desired slow roll. For  $f > 0.1$ , this becomes quite difficult even with the truncation error as small as one part in  $10^{14}$  because the super-inflation phase can become so long that the required evolution spans  $\sim 10^{14} s_{\text{Pl}}$  or more. Therefore, to maintain the precision we had in the kinetic dominated case, another line of reasoning is necessary.

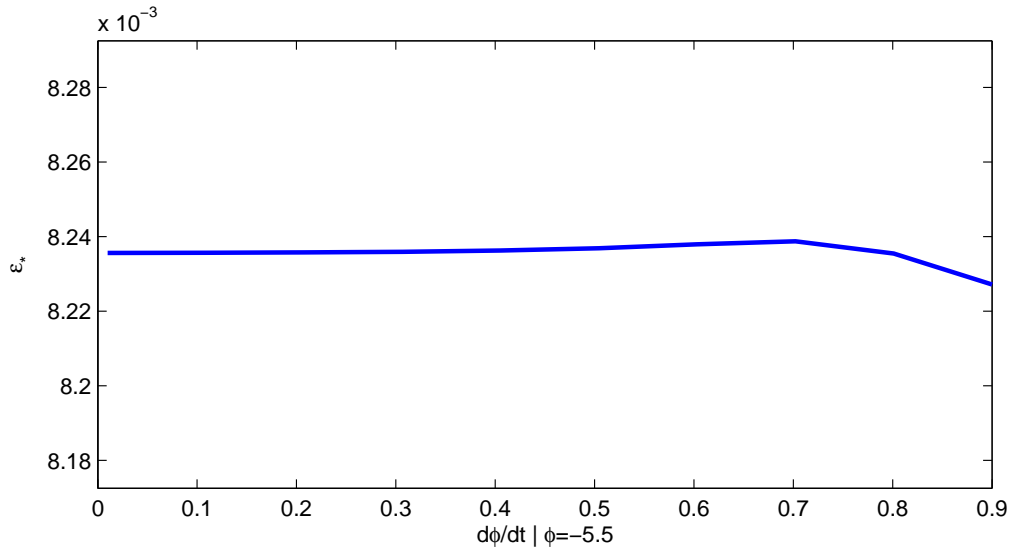


FIG. 3: WMAP data implies that, for a quadratic potential, at the time  $t(k_*)$  at which the reference mode  $k_*$  exits the Hubble horizon,  $|\phi| = 3.15 m_{\text{Pl}}$  and  $\epsilon = 8 \times 10^{-3}$  within error bars of  $\sim 4.5\%$ . We wish to analyze whether generic dynamical trajectories pass through this small neighborhood in the phase space. For reasons discussed in section IV C 2, we consider trajectories with initial data with a fixed, low value of  $\phi$  (which we take to be  $\phi = -5.5 m_{\text{Pl}}$ ), allowing *all* permissible values of  $\dot{\phi}$ . The plot shows that in all the resulting dynamical trajectories, at the time when  $\phi = -3.15 m_{\text{Pl}}$ , we have  $\epsilon \approx 8 \times 10^{-3}$  with fluctuations less than  $2 \times 10^{-5}$ . This implies that *all* LQC trajectories with  $|f| \geq 7.35 \times 10^{-6}$  pass through the desired, small region of the phase space.

Motivated by our result (4.20), in this subsection we consider initial data at the bounce

with  $|\phi_B| \geq 5.5 m_{\text{Pl}}$ .<sup>7</sup> We will first argue that the resulting dynamical trajectory *must pass* through the point with  $|\phi| = 5.5 m_{\text{Pl}}$  with *some* kinetic energy. Since this is a low value of  $|\phi|$ , the inflation will reach the WMAP value  $|\phi| = 3.15 m_{\text{Pl}}$  rather quickly. So it is feasible to carry out a numerical simulation for dynamics between  $|\phi| = 5.5 m_{\text{Pl}}$  and  $|\phi| = 3.15 m_{\text{Pl}}$  with the desired, high degree of accuracy. The question for numerics is then: Is the value of  $\epsilon$  at the time when  $|\phi| = 3.15 m_{\text{Pl}}$  close to the WMAP value  $\epsilon = 8 \times 10^{-3}$  within the 4.5% error bars? For initial data at the bounce for which  $|\phi_B| \gg 5.5 m_{\text{Pl}}$ , the super-inflation phase will last very long time and, had we begun the simulation at the bounce, we would have lost accuracy by the time the inflaton reaches  $|\phi| = 3.15 m_{\text{Pl}}$ . We avoid this problem by giving an *analytic argument* that the inflation *must* reach  $|\phi| = 5.5 m_{\text{Pl}}$  and carry out numerical calculations for dynamics only between  $|\phi| = 5.5 m_{\text{Pl}}$  and  $|\phi| = 3.15 m_{\text{Pl}}$ .

Let us begin with the negative branch of the  $\phi_B$  space, i.e., first consider the case when  $-5.5 m_{\text{Pl}} \geq \phi_B \geq -|\phi_{\text{max}}| = -7.47 \times 10^5 m_{\text{Pl}}$ . In this case, immediately after the bounce the inflaton will roll down the potential. Intuitively, it may seem obvious that in this descent it must encounter the point  $\phi = -5.5 m_{\text{Pl}}$  with *some* kinetic energy. But a priori there are two possibilities that may prevent this occurrence. First, we have to examine the possibility that the inflaton may come to rest for some value  $\phi = \phi_o < -5.5 m_{\text{Pl}}$  and just stops there. But the equation (4.5) satisfied by the inflaton implies that at the instant  $\dot{\phi} = 0$ ,  $\ddot{\phi} = -m^2 \phi_o > 0$  (since  $\phi_o \neq 0$ ). Therefore the inflaton cannot just stay at  $\phi_o < 0$ . A more subtle possibility is that the inflaton asymptotically approaches  $\phi_o < -5.5 m_{\text{Pl}}$ , with  $\dot{\phi}$  approaching zero, but never actually reaches it in a finite time. That is, the limiting value of  $\dot{\phi}$  could be zero at  $\phi = \phi_o$  but this could happen at time  $t_o = \infty$ . But by integrating (4.5) between the bounce time  $t_B$  and the hypothetical time  $t_o$  at which  $\dot{\phi}$  is to vanish, it is easy to show that:

$$t_o - t_B < \frac{|\dot{\phi}_B|}{m^2 |\phi_B|} \quad (4.21)$$

so that  $t_o$  is necessarily finite. Thus, if  $\phi_B < -5.5 m_{\text{Pl}}$  (and by assumption  $\dot{\phi}_B > 0$ ), the inflaton *must* slide down the potential and reach the value  $\phi = -5.5 m_{\text{Pl}}$  with *some* kinetic energy.

Next, consider the case when  $\phi_B > 0$ . In this case, our focus will be on initial data at the bounce with  $\phi_B \geq 5.5 m_{\text{Pl}}$ . Since we again have  $\dot{\phi}_B > 0$ , initially the inflaton now *climbs up* the potential. However, it again follows from (4.5) that it reaches  $\dot{\phi} = 0$  in a finite time  $t_o$  and at that time  $\ddot{\phi} = -m^2 \phi < 0$  (since  $\phi$  is now positive). So this is the turn around point and the inflaton rolls down the potential. Again, by the same reasoning as before, as it rolls down, the inflaton cannot come to rest for a value  $\phi \neq 0$ . Therefore as it rolls down, it must pass through the point  $\phi = 5.5 m_{\text{Pl}}$ , for *some* value of  $\dot{\phi}$ . To summarize, dynamical trajectories for *every initial data at the bounce with  $|\phi_B| \geq 5.5 m_{\text{Pl}}$  eventually encounter a point at which  $|\phi_B| = 5.5 m_{\text{Pl}}$* .

We used high precision numerics to analyze the LQC dynamics following this event. The value of  $\dot{\phi}$  at this event can be arbitrary. We sampled the full range,  $(\dot{\phi} = 0, \dot{\phi} = 0.90 m_{\text{Pl}}^2)$ , first using uniformly distributed *thousand* data points and then logarithmically distributed *thousand* points. Using  $\phi = -5.5 m_{\text{Pl}}$  and each of these values of  $\dot{\phi}$  as initial data solved the full set of LQC equations numerically. The key questions then are: i) Do all these dynamical

---

<sup>7</sup> This space has an overlap with the  $f < 10^{-5}$  case already considered in detail in section IV B. This ensures that there are no ‘gaps’, i.e., we will cover the full space of initial data at the bounce.

trajectories eventually pass through a phase space point at which  $\phi = -3.15 m_{\text{Pl}}$ ; and, ii) Within the WMAP error bars, which of them have  $\epsilon = 8 \times 10^{-3}$  at the time when  $\phi$  assumes the value  $3.15 m_{\text{Pl}}$ ? As one would expect from the analytical considerations discussed above, the answer to the first question is in the affirmative. As the inflaton rolls down the potential from  $\phi = -5.5 m_{\text{Pl}}$ , it necessarily encounters the value  $\phi = -3.15 m_{\text{Pl}}$ . The answer to the second question is summarized in Fig. 3: *in each of these two sets of 1000 simulations*, at the time the inflaton assumes the value  $\phi = -3.15 m_{\text{Pl}}$ , the slow roll parameter  $\epsilon$  takes values in the range

$$\epsilon = 8 \times 10^{-3} \pm 2 \times 10^{-5}. \quad (4.22)$$

That is, each of these trajectories passes through the small portion of the phase space compatible with the WMAP data.

Finally, let us consider the complementary case with initial data at the bounce satisfying  $\phi_{\text{B}} > 5.5 m_{\text{Pl}}$ . In this case, as discussed above, the inflaton first rises up the potential and then rolls down. Therefore now the numerical simulation should start with  $\phi = 5.5 m_{\text{Pl}}$  and  $\dot{\phi} \in (-0.90 m_{\text{Pl}}, 0)$ . But because of the symmetry on the space of solutions noted in the beginning of section IV B, these solutions can be obtained just by reversing the sign of the solutions  $\phi(t)$  obtained from numerical evolutions starting from the initial data  $\phi = -5.5 m_{\text{Pl}}$  and  $\dot{\phi} \in (0, 0.90 m_{\text{Pl}})$ . Thus, all the dynamical trajectories are compatible with the WMAP data also in this case.

To summarize, combining the results of sections IV B 3 and numerical simulations just discussed, we can conclude that the LQC dynamical trajectories resulting from *any* initial data at the bounce surface with  $|\phi_{\text{B}}| \geq 5.5 m_{\text{Pl}}$  realizes the constraints on values of fields at  $t = t(k_*)$  imposed by the WMAP data. Thus, it is only when the bounce is in the extreme kinetic dominated regime that some of the dynamical trajectory —namely those that violate (4.20) can fail to meet the WMAP constraint.

#### D. Probability of the desired slow roll in LQC

We are now ready to combine results of sections III B, IV B and IV C to calculate the a priori probability of realizing the desired slow roll in LQC.

In the terminology of section III B, the event  $E$  of interest is the passage of the dynamical trajectory through the small region in the phase space singled out by the WMAP data and our task is to find the *relative* volume of the region  $R(E)$  of the space of solutions in which  $E$  occurs. The calculation requires a normalized measure. In section III B we found that, thanks to a suitable gauge fixing, each equivalence class of physically distinct LQC solutions can be characterized completely by the value  $\phi_{\text{B}}$  of the inflaton at the bounce surface. Since  $b\lambda = \pi/2$  at the bounce, (3.19) implies that the total measure on the space  $\mathbb{S}_o$  of physically distinct solutions is given by

$$N = \int_{\mathbb{S}_o} \hat{\omega} = \int_{-\phi_{\text{max}}}^{\phi_{\text{max}}} \left( \frac{3\pi}{\lambda^2} - 4\pi^2 \gamma^2 m^2 \phi^2 \right)^{\frac{1}{2}} d\phi = \frac{3\pi}{4\gamma\lambda^2 m} \quad (4.23)$$

where we have used the fact that we have a quadratic potential and where, for definiteness we have set the volume  $v_o$  at the bounce to 1. (Recall that  $v_o$  simply rescales the measure by a constant and therefore drops out in the calculation of probabilities.) The probability

$P(E)$  of the occurrence of our event  $E$  is then given by (3.20):

$$P(E) = \frac{1}{N} \int_{\mathcal{I}(E)} \left( \frac{3\pi}{\lambda^2} - 4\pi^2 \gamma^2 m^2 \phi^2 \right)^{\frac{1}{2}} d\phi \quad (4.24)$$

where  $\mathcal{I}(E)$  is the interval on the  $\phi_B$ -axis corresponding to the physically distinct LQC solutions in which  $E$  occurs. (For details, see section III B.)

In sections IV B and IV C we found that a *sufficient* condition for the event  $E$  to occur is that the initial data of the solution at the bounce should satisfy

$$\phi_B \notin [-5.5 m_{\text{Pl}}, .94 m_{\text{Pl}}] \quad \text{or, equivalently,} \quad f \notin [-7.35 \times 10^{-6}, 1.25 \times 10^{-6}] \quad (4.25)$$

Therefore the probability that  $E$  does *not* occur is bounded by the length of the interval  $[-5.5 m_{\text{Pl}}, .94 m_{\text{Pl}}]$  in the  $\phi_B$ -axis w.r.t. the measure given by the 1-form  $\hat{\omega}$ :

$$\begin{aligned} P(E \text{ not realized}) &\leq \frac{1}{N} \left( \int_0^{\phi_+} + \int_0^{\phi_-} \right) \left( \frac{3\pi}{\lambda^2} - 4\pi^2 \gamma^2 m^2 \phi^2 \right)^{\frac{1}{2}} d\phi \\ &\leq \frac{1}{\pi} (f_+ \sqrt{1 - f_+^2} + \sin^{-1} f_+) + \frac{1}{\pi} (f_- \sqrt{1 - f_-^2} + \sin^{-1} f_-) \\ &\lesssim 2.74 \times 10^{-6} \end{aligned} \quad (4.26)$$

where  $\phi_+ = .94 m_{\text{Pl}}$ ,  $\phi_- = 5.5 m_{\text{Pl}}$  and  $f_{\pm} = \phi_{\pm} / \phi_{\text{max}}$ . Thus, the probability that the desired slow roll does *not* occur in an LQC solution is *less than three parts in a million*. Hence a great deal of fine tuning would be necessary to avoid the slow roll inflation that meets the WMAP constraints.

For simplicity, throughout our analysis, we set the cosmological constant  $\Lambda$  to be zero. But it is completely straightforward to include it since it just shifts the zero of our potential. Since the sign of the observed cosmological constant is positive, for any given value of  $\phi$ , its inclusion would have the effect of increasing the fraction of the total energy density in the potential. This in turn would *lower* the values of  $|\phi_B|$  that are needed in (4.20) to ensure that the trajectory meets the WMAP constraint. Thus the probability of achieving the desired slow roll would further increase. However, since the observed value of  $\Lambda$  is so small, this effect will not be noticeable even at the level of numerical accuracy used in this paper. We also focused on the spatially flat FLRW models because they are observationally favored. But it is not difficult to include spatial curvature. Again, given observational constraints, we expect that this inclusion will not significantly alter our main conclusions [34]. In these respects, the results are robust.

What about the choice of the inflaton potential? All our detailed considerations hold only for a quadratic potential. Recall however that a generic potential  $V(\phi)$  is well-approximated by a quadratic one near its minimum. Suppose  $V(\phi)$  has a single minimum  $\phi_o$  and that  $|V(\phi) - V(\phi_o) - (1/2)m^2\phi^2| \ll V(\phi) - V(\phi_o)$  for all  $\phi \in [-5.5 m_{\text{Pl}}, 5.5 m_{\text{Pl}}]$  where  $m \approx 1.21 \times 10^{-6} m_{\text{Pl}}$ . Then our considerations will apply: As the inflaton slides down from  $|\phi| = 5.5 m_{\text{Pl}}$  it will enter a phase of slow roll inflation compatible with the WMAP constraints. As an illustration, let us suppose that the potential is a combination of a quadratic and a quartic parts:

$$V(\phi) = \frac{1}{2} m^2 \phi^2 + \frac{\lambda}{4} \phi^4 \quad (4.27)$$

Then, our assumption is met if  $\lambda \ll 9.68 \times 10^{-14}$ . For a rough comparison, note that the WMAP bound for a pure quartic potential is  $4.4 \times 10^{-14}$ . Thus, it is not unreasonable to expect that, at a qualitative level, our conclusions on probabilities will continue to hold for a wide class of physically interesting potentials.

## V. DISCUSSION

In the main body of this paper we analyzed inflation in the observationally most interesting case of the  $k=0$  FLRW cosmologies using the framework of LQC. Our goal was two-fold. First, assuming a quadratic potential, we examined in detail the effective LQC dynamics in presence of an inflaton with standard potentials. Second, we used this dynamics to calculate the *a priori* probability of realizing the desired slow roll inflation that is compatible with the WMAP data.

Let us begin with dynamics. Since the big bang singularity is replaced by the big bounce, and since all physical fields are regular at the bounce, we could specify initial conditions at the bounce surface and explore the resulting dynamics. We allowed *all possible* initial data, subject only to the Hamiltonian constraint. We found that the subsequent dynamics is sensitive to the distribution of energy density at the bounce between kinetic and potential parts. In all cases, there is a universal super-inflation phase that follows the bounce; indeed it persists even when there is no potential at all. For concreteness, let us focus on the case when  $\dot{\phi}$  and  $\phi$  are both positive at the bounce so the inflaton is climbing up the potential.

We first discussed in detail the case in which less than one part in  $10^{10}$  of the total energy density at the bounce is in the potential because this is the only case in which some of the solutions can fail to exhibit the desired slow roll. In this case, the super-inflation phase is very short lived. However, it is also extremely dynamic: during the fraction of a Planck second of super-inflation, the Hubble parameter increases dramatically from zero to its *maximum allowed value*,  $0.93 m_{\text{Pl}}$ . Because  $H$  is so large at the end of super-inflation, the friction term in the equation of motion of the inflaton is also large whence the inflaton loses kinetic energy as it climbs up the potential. After  $\sim 10^4 s_{\text{Pl}}$ , the potential energy equals kinetic energy and then dominates it (where, as before,  $s_{\text{Pl}}$  denotes Planck seconds). After another  $\sim 10^4 - 10^5 s_{\text{Pl}}$ ,  $\dot{\phi}$  vanishes, the inflaton turns around and starts climbing down the potential. In a ‘majority’ of solutions—but not all—it soon enters the desired slow roll that is compatible with the 7-year WMAP observations [6].

In the intermediate case, the kinetic energy is still greater than the potential at the bounce but does not overwhelm it. Now dynamics undergo the same qualitative phases. However, the super-inflation phase lasts a bit longer and the turn around occurs much sooner, only about  $10 - 100 s_{\text{Pl}}$  after the bounce. This is because the initial kinetic energy is smaller than that in the first case while the strength of the friction term is the same because the Hubble parameter again takes its maximum value at the end of super-inflation. Because the turn around occurs much sooner, in contrast to the situation in the extreme kinetic domination, the increase in the value of  $\phi$  between the bounce and the turn-around is very small. Finally, if the potential energy density exceeds the kinetic energy density at the bounce, dynamics is very different. Now the LQC effects dominate in the sense that the super-inflation phase lasts longer and its duration increases rapidly as the fraction of total energy in the potential increases. Furthermore, the turn around occurs already during super-inflation! Our first goal was to present these qualitative differences in the pre-slow-roll dynamics.

The WMAP data puts very strong constraints on the values of fields at the time  $t(k_*)$  when the mode with wave number  $k_*$  exits the Hubble radius during the desired phase of inflation. The key question is: Are ‘most’ dynamical trajectories such that these constraints are met at *some* time during the post-bounce evolution? We showed that the answer is in the affirmative unless the bounce is kinetic energy dominated as in section IV B. Even in this case, the WMAP constraints are met unless fraction of the total energy at the bounce

which is in the potential is less than  $7.35 \times 10^{-6}$ . In this precise sense the tiny region of phase space selected by the WMAP data serves as an *attractor* to LQC dynamics. This may not seem surprising because inflationary trajectories are known to be attractors also in general relativity. However, in LQC there are strong quantum gravity effects in the super-inflation phase as well as in the phase that follows immediately after super-inflation. These could well have spoiled the attractor behavior and a large fraction of the data *specified at the bounce* could well have given rise to trajectories that steer away from the WMAP region. That this does not happen is noteworthy.

The attractor behavior is a qualitative feature of dynamics. It does not provide a sharp *quantitative* estimate on the likelihood of realizing the desired slow roll. To obtain this estimate, one needs a *measure* on the space of (physically distinct) solutions, such that the total volume of this space is finite. As explained in section I, a natural strategy [7–9] is to use the Liouville measure on the phase space. This leads to *a priori* probabilities of events, such as the occurrence of the desired slow roll. However, volume of the 2-dimensional space  $\mathbb{S}$  of solutions with respect to the resulting  $d\hat{\mu}_L$  is infinite. But this infinity is physically spurious: It occurs because  $\mathbb{S}$  is acted upon by a gauge group  $\mathcal{G}$  and the length of 1-dimensional orbits of  $\mathcal{G}$  is infinite. For a large class of potentials the space  $\mathbb{S}/\mathcal{G}$  of physically distinct solutions is in fact a *bounded* interval of the real line. Furthermore there is a natural 1-form  $\omega_\alpha$  on  $\mathbb{S}$  (constructed from the symplectic structure and the gauge vector field  $G^\alpha$ ) which is everywhere orthogonal to  $G^\alpha$ . So it is a natural candidate to induce a volume element on the 1-dimensional space  $\mathbb{S}/\mathcal{G}$ . Unfortunately, it does not project down to  $\mathbb{S}/\mathcal{G}$  (because  $\mathcal{L}_G \omega_\alpha = \omega_\alpha \neq 0$ ). Therefore one is led, instead, to ‘fix a gauge’, i.e., lift  $\mathbb{S}/\mathcal{G}$  to a suitable 1-dimensional cross-section in  $\mathbb{S}$  and carry out integration there. The problem in general relativity is that there is no natural family of lifts and the volume element on  $\mathbb{S}/\mathcal{G}$  depends heavily on one’s choice. Thus, there is an inherent ambiguity in the calculation of probabilities. Thanks to the existence of the bounce surface, in LQC one does have a natural family of lifts and the probability of occurrence of physical events is independent of the choice.<sup>8</sup> We used this choice to calculate the a priori probability of realizing the desired slow roll, compatible with the WMAP data. We found that the probability is *greater than* 0.999997 in LQC. As emphasized in section I, these are just ‘bare probabilities’ and better estimates of this occurrence will require astutely chosen physical inputs. This will require not only a more complete theory [3], but a deep understanding of that theory to separate essential inputs from non-essential ones. However, since the ‘bare probability’ is so close to 1, it is a huge burden on any theory to come up with new inputs that significantly change the answer.

We emphasize, however, that our results should not be interpreted to mean that sufficiently long slow roll inflation is inevitable in LQC: it is inevitable *only* under the additional assumption that there is a phase in which matter density is dominated by that of a scalar field in a suitable potential. So far LQC has not provided a mechanism to create either the scalar field or the potential. Although there have been intriguing suggestions that this may naturally occur if one promotes the Barbero Immirzi parameter  $\gamma$  of loop quantum gravity

---

<sup>8</sup> In this construction, the analog of the bounce surface in general relativity would be the singularity itself. It is far from obvious how to work at the singularity although ideas proposed in [35] may provide a natural mathematical construction. However, a priori, the physical meaning of such a construction would be obscure because one would have to assume that Einstein’s equations, without quantum corrections, are valid all the way to the singularity.

to a dynamical field [36], very substantial work is needed to have confidence that they can be transformed into a concrete, internally complete and viable scenario.

The primary purpose of our analysis was to understand what LQC has to say about inflationary scenarios in the early universe. But it is instructive to compare and contrast the predictions of LQC with those of general relativity, discussed in the literature. This leads us to several distinct points. First, there is some controversy as to which ‘problems’ inflation solves and which it does not [1–3]. Our analysis does not shed any new light on these issues. Rather, as mentioned above, our focus is on the likelihood of the desired slow roll inflation. Second, while some of the literature [4, 7–9] uses the Liouville measure on the space of solutions to compute the a priori probability, in [2] (and in the earlier literature cited therein) a different measure is used. The likelihood, of course, can and does depend sensitively on the choice of the measure. In addition, since the choice made in [2] is not preserved by the Hamiltonian flow, a choice of time slice is made. Therefore, there is some discussion in the literature on the dependence of the final results on the choice of the measure and the time slice used in the evaluation of probabilities (see, e.g., [1, 3, 4]). The Liouville measure is ‘canonical’ and, furthermore, preserved under time evolution. However, as explained above, the total measure on the space of solutions  $\mathbb{S}$  is infinite and, to extract meaningful probabilities, one must introduce an additional structure, a suitable lift of  $\mathbb{S}/\mathcal{G}$  into  $\mathbb{S}$ . Conceptually, this is equivalent to fixing a ‘time gauge,’ e.g. by working with the initial data of the solution at the instant at which the matter density is a given constant,  $\rho_o$ . In this sense, there is a common limitation. In [2] (and in earlier works dating back to [32]) one uses the time slice at Planck time (but still works with equations of general relativity), while in [4] it is argued that one should use a slice corresponding to a *much* later time. Even if one were to decide to use the Liouville measure, a priori probabilities do depend sensitively on this choice because of the nature of inflationary dynamics [10]. From our perspective, since there is no ‘canonical’ choice of time slice in general relativity, calculations of probabilities have an inherent ambiguity.<sup>9</sup> In LQC, by contrast, since the bounce surface provides a canonical ‘time slice’ the ambiguity can be naturally resolved. Finally, recently there have been several interesting discussions of inflationary scenarios in LQC (see, e.g., [37–42]). However, the primary focus of all but one of these papers is on phenomenological and observational issues rather than on measures and calculations of probabilities. The one exception is [37]. However, in that reference, super-inflation (as well as the bounce) was ignored.

We will conclude with an observation on dynamics immediately following the bounce. In the standard inflationary scenarios, matter density is some 11-12 orders of magnitude smaller than  $\rho_{\text{Pl}}$  at the onset of inflation and from the quantum equations of full LQC we know that the use of quantum field theory in curved space-times is fully justified in this regime. However, there are several conceptually important issues which require an understanding of dynamics *before* this era is reached. Perhaps the most important among them is the issue of the initial state of quantum fields representing perturbations. As explained in section I, currently the state is simply postulated to be the Bunch-Davis vacuum for the relevant modes (which have co-moving wave numbers in the range  $(k_o, \sim 200k_o)$ ). While this assumption

---

<sup>9</sup> There is another difference between references [2] and [4]: while [2] focuses on the (phenomenologically favored)  $k=0$  model, [4] focuses on the (spatially closed)  $k=1$  model. However, since the strategy used in [4] to ‘regularize’ the Liouville measure is strongly motivated by the gauge considerations in the  $k=0$  case, this difference is less significant for the drastic disparity in the final results.

is physically motivated, it is nonetheless important to arrive at this state starting from more fundamental initial conditions. In general relativity, these conditions would have to be specified on the singularity and furthermore we know that we cannot reliably use equations of general relativity in the Planck regime. LQC on the other hand is based on loop quantum gravity, a candidate theory of full quantum gravity. Therefore, not only is there a basis to trust its quantum equations but, as we saw in section II, they have already provided us a wealth of new information on physics at the Planck scale. Therefore, there is good motivation to use quantum field theory on the cosmological *quantum space-times* of LQC [43] to study the initial conditions and evolution of quantum fields representing perturbations from the big bounce until the onset of inflation. Is there perhaps a natural initial condition we can impose on the quantum state of these perturbations at the bounce using e.g., ideas developed in [44] and/or exploiting the fact that the Hubble parameter vanishes there? What would such an initial state evolve to at the onset of slow roll? Would it be sufficiently close to the Bunch-Davis vacuum (for the modes of interest) to be phenomenologically viable, or, would it be so different that it is already ruled out observationally? If it close, is it perhaps too close to be observationally indistinguishable from the Bunch-Davis vacuum or is it sufficiently different to lead to an observational test of LQC? These questions are being currently analyzed using the detailed dynamics of the LQC inflationary space-times presented in section IV B [17].

Finally, because almost all LQC solutions are compatible with the WMAP data, one might first think that the chances of constraining quantum gravity from observations of the early universe are very small. However this is not correct: to make contact with these observations one needs not only the ‘background’ space-time but also quantum fields representing perturbations off this background. Considerations of the previous paragraph suggest a concrete direction to confront quantum field theory on the LQC quantum space-times with observations. Such a confrontation could well lead to interesting, testable predictions of loop quantum gravity and/or constraints on this theory.

### Acknowledgments

We would like to thank Ivan Agullo, Alejandro Corichi, Neil Turok and William Nelson for discussions. This work was supported in part by the NSF grant PHY0854743 and the Eberly and Frymoyer research funds of Penn State.

- 
- [1] S. Hollands and R.M. Wald, An alternative to inflation, *Gen. Rel. Grav.* **34**, 2043 (2002);
  - [2] L.A. Kofman, A. Linde and V.F. Mukhanov, Inflationary theory and alternative cosmology, *J. High Energy Phys.* **10**, 057 (2002)
  - [3] S. Hollands and R.M. Wald, Comment on Inflation and Alternative Cosmology [arXiv:hep-th/021000](#)
  - [4] G.W. Gibbons and N. Turok, The Measure Problem in Cosmology, *Phys. Rev. D* **77**, 063516 (2008)
  - [5] A. Ashtekar and D. Sloan Loop Quantum Cosmology and Slow Roll Inflation, *Phys. Lett. B* **694**, 108-112 (2010), [arXiv:0912.4093](#) 200911



- [6] E. Komatsu et al, Seven-Year Wilkinson microwave anisotropy probe (WMAP) Observations: Cosmological interpretation, [arXiv:1001.4538](#)
- [7] G. W. Gibbons, S.W. Hawking and J. Stewart, Nucl. Phys. **B281**, 736 (1987)
- [8] D.N. Page, Phys. Rev. D. **36**, 1607 (1987)
- [9] S. W. Hawking and D. N. Page, Nucl. Phys. **B298**, 789 (1988)
- [10] A. Corichi and A. Karami, On the measure problem in slow roll inflation and loop quantum cosmology, [arXiv:1011.4249](#)
- [11] A. Ashtekar, T. Pawłowski and P. Singh Quantum Nature of the Big Bang Phys. Rev. Lett. **96** 141301 (2006)
- [12] A. Ashtekar, T. Pawłowski and P. Singh, Quantum nature of the big bang: Improved dynamics, Phys. Rev. **D74**, 084003 (2006)
- [13] A. Ashtekar, T. Pawłowski, P. Singh and K. Vandersloot Loop Quantum Cosmology of  $k=1$  FRW models Phys. Rev. **D75** 024035 2007
- [14] E. Bentivegna and T. Pawłowski, Anti-deSitter universe dynamics in LQC, Phys. Rev. **D77**, 124025 (2008)
- [15] A. Ashtekar, A. Corichi and P. Singh, Robustness of key features of loop quantum cosmology, Phys. Rev. **D77**, 024046 (2008)
- [16] A. Linde, Inflation and String Cosmology, Prog. Theor. Phys. Suppl. **163** 295-322 (2006)
- [17] I. Agullo, A. Ashtekar and W. Nelson, (in preparation)
- [18] A. Ashtekar and J. Lewandowski Background Independent Quantum Gravity: A Status Report Class. Quant. Grav. **21** R53 2004
- [19] C. Rovelli, *Quantum Gravity*. (Cambridge University Press, Cambridge (2004))
- [20] T. Thiemann, *Introduction to Modern Canonical Quantum General Relativity*. (Cambridge University Press, Cambridge, (2007))
- [21] A. Ashtekar, J. Baez, and K. Krasnov, Quantum Geometry of Isolated Horizons and Black Hole Entropy, Adv. Theor. Math. Phys. **4**, 1-94 (2000)
- [22] I. Agullo, J. Fernando Barbero G., E. F. Borja, J. Diaz-Polo, E. J. S. Villaseñor, Detailed black hole state counting in loop quantum gravity Phys. Rev. **D82**, 084029 (2010)
- [23] M. Bojowald Absence of Singularity in Loop Quantum Cosmology Phys. Rev. Lett. **86** 5227 (2001)
- [24] A. Ashtekar and E. Wilson-Ewing Loop Quantum Cosmology of Bianchi I Models Phys. Rev. **D79** 083535 (2009)
- [25] A. Ashtekar and E. Wilson-Ewing Loop Quantum Cosmology of Bianchi Type II Models Phys. Rev. **D80** 123532 (2009)
- [26] E. Wilson Ewing, Loop quantum cosmology of Bianchi type IX models, Phys. Rev. **D82**, 043508 (2010)
- [27] G. Mena Marugan and M. Martin-Benito Hybrid Quantum Cosmology: Combining Loop and Fock Quantizations Int. J. Mod. Phys. **A24** 2820 2009
- [28] V. Taveras Corrections to the Friedmann Equations from LQG for a Universe with a Free Scalar Field Phys. Rev. **D78** 064072 2008
- [29] P. Singh Are Loop Quantum Cosmos Never Singular? Class. Quant. Grav. **26** 125005 2009
- [30] A. Ashtekar, Loop Quantum Cosmology: An Overview, Gen. Rel. Grav. **41**, 707-741 (2009); The big bang and the quantum, AIP Con. Proc. 1241:109-121.2010, edited by J-M Alimi and A. Füzfa, [arXiv:1005.5491](#)
- [31] P.S. de Laplace, *Théorie analytique des probabilités* (Courcier, Paris, 1812); *A philosophical essay on probabilities*, translated by A. I. Dale, (Springer, New York, 1995)

- [32] V. A. Belinsky, I. M. Khalatnikov, L. P. Grishchuk and Y. B. Zeldovich, Inflationary Stages In Cosmological Models With A Scalar Field, *Phys. Lett. B* **155** 232 (1985)
- [33] A. R. Liddle, P. Parson and J. D. Barrow, Fomalalising the slow roll approximation in inflation, *Phys. rev. D* **50** 7222-7232 (1994)
- [34] D. Sloan (in preparation)
- [35] S. Foster, Scalar field cosmologies and the initial space-time singularity, [arXiv:gr-qc/9806098](#)
- [36] V. Taveras and N. Yunes The Barbero-Immirzi Parameter as a Scalar Field: K-Inflation from Loop Quantum Gravity? *Phys. Rev. D* **78** 064070 2008
- [37] C. Germani, W. Nelson and M. Sakellariadou, on the onset of inflation in loop quantum cosmology, *Phys. Rev. D* **76**, 043529 (2007)
- [38] J. Grain, A. Barrau, Cosmological footprints of loop quantum gravity, *Phys. Rev. Lett.* **102**, 081301 (2009)
- [39] J. Grain, T. Cailleteau, A. Barrau and A. Gorecki, Fully Loop-Quantum-Cosmology-corrected propagation of gravitational waves during slow-roll inflation; *Phys. Rev. D* **81** 024040 (2010)
- [40] J. Grain, A. Barrau, T. Cailleteau, J. Mielczarek, Observing the Big Bounce with Tensor Modes in the Cosmic Microwave Background: Phenomenology and Fundamental LQC Parameters, *Phys. Rev. D* **82** 123520 (2010)
- [41] J. Mielczarek, T. Cailleteau, J. Grain, A. Barrau, Inflation in loop quantum cosmology: Dynamics and spectrum of gravitational waves, *Phys. Rev. D* **81** 104049 (2010)
- [42] A. Barrau, Inflation and Loop Quantum Cosmology, [arXiv:1011.5516](#)
- [43] A. Ashtekar, W. Kaminski and J. Lewandowski, Quantum field theory on a cosmological, quantum space-time, *Physical Review D* **79**, 064030 (2009), [arXiv:0901.0933](#)
- [44] J. Cortez, G. A. Mena Marugan, J. Olmedo and J. M. Velhinho, A unique Fock quantization for fields in non-stationary spacetimes, *JCAP* **1010** 030 (2010);  
Uniqueness of the Fock quantization of fields with unitary dynamics in nonstationary spacetimes, *Phys. Rev. D* **83** 025002 (2011)